TÉCNICO LISBOA

A NEW DEFORMATION-ASSISTED JOINING PROCESS FOR FIXING SHEETS TO TUBES

Experimental and Numerical Analysis

Frederico José de Lacquet Rocha e Silva

Thesis to obtain the Master of Science Degree in

Mechanical Engineering

Supervisors: Prof. Luís Manuel Mendonça Alves
Eng. Rafael Augusto Nunes Miranda Malta Afonso

Examination Committee

Chairperson: Prof. Rui Manuel dos Santos Oliveira Baptista
Supervisor: Eng. Rafael Augusto Nunes Miranda Malta Afonso
Members of the Committee: Prof. Ivo Manuel Ferreira de Bragança
Eng. João Pedro da Fonseca Matos Pragana

September 2019

Acknowledgments

Firstly, I'd like to thank my supervisors, Professor Luís Alves and Eng. Rafael Afonso, for the continuous support given and the true inspiration they were on this important step of my journey. The constant idea that in order to achieve better results, something different must be done is a thought I'll carry with me indefinitely. Thank you for the knowledge, experience and enthusiasm, without it this wouldn't have been possible.

To Professor Paulo Martins, for being an example and a true inspiration. The support and guidance given to me cannot be put into words. I thank you for having had the opportunity to work alongside you and learn from someone that, for me, represents everything a professor and researcher should be.

To Pai, Mãe, Leonor, Oma, Opa, Avó, Tia, Tante Bénédicte, Nonkel Karel, Tante Carla, Nonkel Filip, for being there for me and helping me through the toughest times life has presented me, and for being my favourite company to celebrate the good ones. It's thanks to you I was able to get where I am today. To Jacques, Evelyne, Thomas, Philippe, Katrin, Charline, Manon, the best cousins I could ask for. Thank you for making this journey so special for me and showing me unconditional support wherever, whenever. To my family.

To Tia Leonor, Verónica, Paula for being family since the day I was born. Thank you so much for guiding me through life and always being an example for me.

To Francisco, Graça, João, Tunes. It's been truly thrilling to share this life chapter with you and I can't put into words how much I'm thankful for everything each and everyone of you has done for me. For being there in the highs and lows, I truly wish the very best for you. Thank you for having given me the opportunity to share these 5 years with you. It's been a pleasure boyz.

To Manel, Bernardo, Nelson, João Pedro, Fonseca, Ricardo, Tété, Carolina, Madalena and Inês. Your friendship to me is something that can never be repaid and I thank you for all of the experiences that we shared that led to this important moment of my life. Without you it wouldn't have happened.

To Stef and Amar. My life in Belgium couldn't have been better accompanied and I have you to thank for making that experience so special for me.

Abstract

This dissertation proposes a new concept for a joining by forming process for joining sheets to tubes away from the tube's end. The sheet-tube connection is obtained by squeezing the sheet adjacent to the outer tube radius, instead of applying direct loading on the tube itself as it was done before in the previous joining by forming processes. The development compares both experimental and finite element modelling results in order to identify the main operating parameters. A deep understanding of their influence in plastic flow allows to characterize the different modes of deformation leading to acceptable and unacceptable joints. Utilization of a deformation-zone geometry parameter to characterize plastic flow inside sheet thickness leads to the conclusion that combination of inhomogeneous and homogeneous deformation through the squeezing depth is necessary for obtaining sound joints with good pull-out destructive forces. Further investigation regarding the influence of the squeezing depth on the joint's performance and the interdependence between the main parameters will allow for the validation of the concept. Moreover, further investigation was made in relation to the new surface formation mechanism, the forces involved in the process and some characteristic behaviours found in this new technique such as the excessive sheet bending.

Keywords

Joining by forming, Sheets, Tubes, Experimentation, Finite element modelling

Resumo

A presente dissertação propõe uma nova união de componentes por deformação plástica, em particular, é proposta uma nova solução que visa a ligação mecânica de tubos e chapas longe da extremidade do tubo. A ligação é obtida comprimindo a chapa na região adjacente ao raio exterior do tubo, ao invés da aplicação de carga ocorrrer diretamente no tubo, como acontecia em soluções anteriores. O desenvolvimento deste novo conceito compara resultados obtidos de forma experimental e de forma numérica (através de simulação por elementos finitos) e dessa forma são conhecidos os parâmetros principais de operação deste processo. Consequentemente, é efectuado um estudo mais aprofundado que visa discriminar os vários modos de deformação obtidos por variação destes parâmetros principais do processo. É visto que a criação de vários modos de deformação irá influenciar o comportamento do escoamento de material e, dependendo desse comportamento, irão resultar ligações consideradas aceitáveis e inaceitáveis. Os diferentes modos de deformação foram caracterizados usando um parâmetro denominado ”deformation-zone geometry parameter” e dessa forma foi permitido a concluir que, de facto, uma mistura de deformação completamente homogénea e não homogénea ao longo da profundidade de compressão é chave para serem obtidas ligações aceitáveis e que suportam elevadas cargas de separação. Estudos adicionais foram efectuados com o intuito de ser entendida a influência da profundidade de compressão na carga de destruição da ligação e a interdependência entre estes dois parâmetros principais. Para além disso, mais investigação foi feita relativamente ao mecanismo de formação de novas superfícies, forças envolvidas no processo e comportamentos característicos desta nova técnica como a deformação excessiva da chapa.

Palavras Chave

União por Deformação Plástica, Chapas, Tubos, Experimentação, Modelação por Elementos Finitos

Contents

List of Figures

List of Tables

Listings

l - Cross-Section Recess Length

d - Squeezing Depth

α - Contact Surface Angular Incline

ϕ - Lateral Surface Angular Incline

t_0 - Tube Thickness

t_s - Sheet Thickness

r_0 - Tube Inner Radius

r_b - Tube Inner Bead Radius

h - Squeezing Punch Indentator Length

s_L - Sheet Length

Δ - Deformation-Zone Parameter

f_m - Friction Coeficient between Materials

f_d - Friction Coeficient between Materials and Dies

t_i - Time Increment between Steps

1

Introduction

Contents

1.1 Contextualization and Motivation

Numerous challenges are presented to engineering on a daily basis and in nowadays, serious concerns regarding the environment force innovation to find new solutions that achieve results in a cleaner fashion. As was said by the company Trumpf: "Manufacturing sustainability and resource efficiency have become important topics for industry and research. New legal requirements such as the EU's Ecodesign Directive (2009/125/EC) set clear markers for the future." [1].

In the production of every structure, joining of a certain amount of components is necessary. Tubes and sheets don't live alone and are usually combined for producing improved products or structures.

Looking to today's context, it's evident that in order to join components, the most used techniques relate to either mechanical fasteners or welding technologies. However, these two conventional techniques bring certain problems, mainly in areas related to environmental impacts and structural performance, for example, the use of mechanical fasteners adds a lot of weight to structures.

In a study performed by the company Trumpf [1], the environmental impact of the use of welding technologies was studied having in consideration factors such as: impact on the ozone layer through photochemical reactions between ozone and welding gases, acidification potential among other harming effects. Most common welding techniques are known to be responsible for an enormous amount of pollution and potential global warming effects.

To tackle these problems and as will be seen further in the State of the Art review, a lot of research and development has been done recently in order to develop new processes that produce the same joints in a cleaner and cheaper fashion, without compromising the performance of the structures. These new processes are part of a new field of study designated as Joining by Forming. Despite the many advantages of these new joining processes, two main problems still arise:

- Most techniques still require multiple separate operations, which in turn increases lead times and difficults the industrial application of these new technologies.

- The techniques that were developed to be successful in a single operation, cannot be used in materials with low fracture toughness, which limits the applicability and industrial integration of these processes.

However, this dissertation will overtake these two issues by looking at all the recent Joining by Forming technologies in a different way that will allow for an easier production of joints whose applicability in industries such as the automotive industry (fabrication of frames for the chassis of the automobile) and heat exhangers is enormous, as seen in [2].

1.2 Objectives

The main objectives of this dissertation are to define and study the main operating parameters of a process that has never been tried before.

Through experimental testing and numerical simulation, the new concept can be validated in order for it to be industrially implemented. A wide variety of different studies were performed to reveal the application window associated to this new technique.

Another objective of this dissertation is to deeply comprehend the improvements achieved when compared to existing technologies and the limitations associated with this new concept that will motivate future research.

1.3 Dissertation Structure

This dissertation is divided in 7 chapters. It starts with the Introduction chapter, where a brief contextualization of the problem is made and the main goals of the dissertation are presented.

In chapter 2, a State of the Art Review will be offered where the evolution of the many techniques will be shown, referring the main advantages and disadvantages, which led to the creation of this new process.

In chapter 3, an overview of all the experimental development will be made. All the types of experimental tests made, the equipment used and the procedures followed will be presented.

In chapter 4, the numerical development will be discussed and the main simulation parameters will be studied in depth.

In chapter 5, a comparison between experimental and numerical results will allow the extensive comprehension of all the advantages offered by this new process. The concept is validated in this chapter as deep conclusions of its functionality and versatility are shown.

In chapter 6, applications of the same technology in different materials are shown to prove its effectiveness across a wide range of materials.

In chapter 7, the main drawn conclusions of the dissertation are presented,future work possibilities are discussed to open doors for the continuous improvement of this new technology.

2

State of the Art

Contents

In this chapter, a review will be made on the main technologies used to perform the joining of sheets to tubes. The state of the art analysis will be split in two distinct parts as a clear distinction can be made between the conventional used technologies (such as welding, mechanical fastening and adhesive bonding) and the technologies more recently promoted that make use of plastic deformation and designated as Joining by Forming or Deformation-Assisted Joining.

2.1 Conventional Technologies

2.1.1 Mechanical Fastening

With the use of bolts, nails, rivets and others, mechanical joints between components are easily obtained. These connections result from the direct interference between the surface of both connector and joined material and the large friction that is created between the joined components. One of the main advantages of the use of this type of technology (in the case of bolt fastening) is the fact that the resulting connection isn't permanent, allowing both quick assembly and disassembly without altering any material or component properties. Another big advantage relates to the fact that this technology allows for joining of dissimilar material at low cost. However, this type of connections have a big disadvantage of allowing a large stress concentration to appear on the connected spots which might lead to failure in some cases. Also, in applications where the structural weight is an important decision factor, the added weight introduced by the joining material does not provide the best results. Another problem with this type of connection is the poor sealing that could cause some corrosive damage to connections.

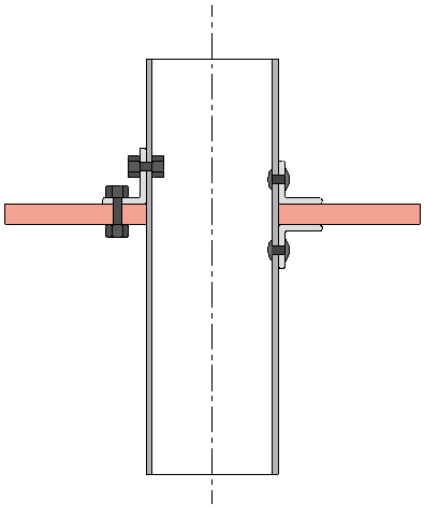

Figure 2.1: Joining by mechanical fastening: through bolts on the left side and trough rivets on the right side.

2.1.2 Adhesives and Welding

Another type of technology widely used in current industry for the joining of structural components, namely tubes and sheets, is the chemical joining. These connections are obtained by making use of structural adhesives and for that reason, another used designation for this technology is adhesive bonding. Joints performed by this type of procedure result from chemical reactions between the surfaces of the used adhesive, which must be chosen according to the materials that are wished to be joined. A big advantage drawn from the use of this type of joining technique is the non-existence of regions with large stress concentrations, as seen above with mechanical fastening.

Because the chemical reactions are what determine the connection, the larger the area where an adhesive is acting, the bigger the joint resistance, which means it's not appropriate for certain applications where a limited connection area is available and a large resistance is required. Other disadvantages come from the necessity of performing a thorough surface preparation before an adhesive is applied and the necessity of having a cleaner environment as contamination by non proper surface preparation or aggressive atmosphere could imply weaker joints and different chemical reactions and also, long cure times are usually needed with these processes.

A good advantage of this technique lies on the fact that neither material properties or micro structures are altered throughout the process, providing thus a benefit that other joining processes can´t offer.

Welding is done at the atomic level, by altering material properties and enabling attractions between atoms and molecules. It is applied not only to metals but also to ceramics and polymeric materials, offering a faster solution to both adhesive bonding and mechanical fastening. The ability to join a numerous amount of materials and being an easily automated technique turned it into one of the most used technologies worldwide. However, some problems arise with the use of this technique such as difficulties in joining dissimilar materials, residual stresses and the necessity of using clamps and jigs to prevent distortions arising from the thermal expansion-contraction cycles that pose great challenges for the technology.

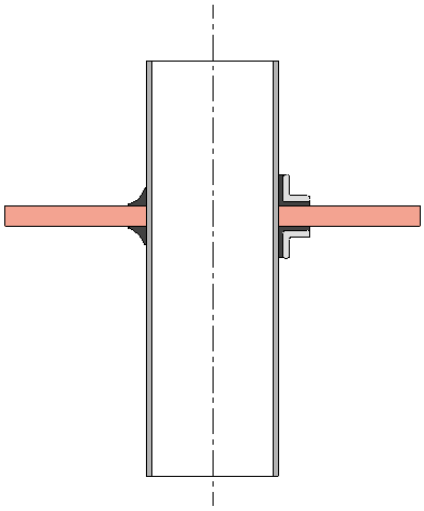

Figure 2.2: Joining through welding on the left side and joining through adhesives on the right side.

In order to overcome all the problems mentioned above, the development of technologies that allow for the joining a wider range of materials in a cleaner and easier way than the techniques above are presented.

2.2 Joining by Forming Review

Connections made by joining by forming technologies revealed themselves as a solution that could provide sounds connections in a sustainable way, being more environmentally friendly while not influencing their performance and aesthetic quality.

In 2014, revisions on these processes were made by both Mori et al. [3] and Groche et al. [4] which stated the large flexibility provided by the joining by forming processes and therefore easily allowed the creation of very complex structures. Virtually all materials can be joined (even dissimilar materials) if joining parameters respect the material's properties and for large production series, joining by forming technologies provide a quicker and cheaper solution, while at the same time having a tremendous dimensional accuracy and repeatability.

More recently, Alves et al. [5] revised all the developments made until 2018 in these types of joining by forming technology, offering a broader variety of applications and processes than offered until that point. A clear distinction was made between the various techniques, splitting joining by forming processes in two main categories, interfacial pressure and mechanical interlock. In this review, the processes shown applied to tube to tube, sheet to sheet and sheet to tube connections.

In the following sections, a summary of the different joining by forming processes using interfacial

pressure and mechanical interlock mechanisms will be presented to show their evolution throughout time and be able to introduce the new joining technique developed during this thesis.

2.2.1 Interfacial Pressure Joining Development

In 2008, Matsumoto et al. [6] proposed a method of plastic joining of sheets to tubes that based its nature on interfacial pressure. This means that the connection is assured by the pressure in the contacting interfaces after thermal expansion-contraction cycles. As seen in the pictures below (Figure 2.3), an indentation is made to a hot forged sheet using a cold bar. After the indentation is concluded, the cooling of the sheet assures a clinching mechanism that maintains the resulting joint.

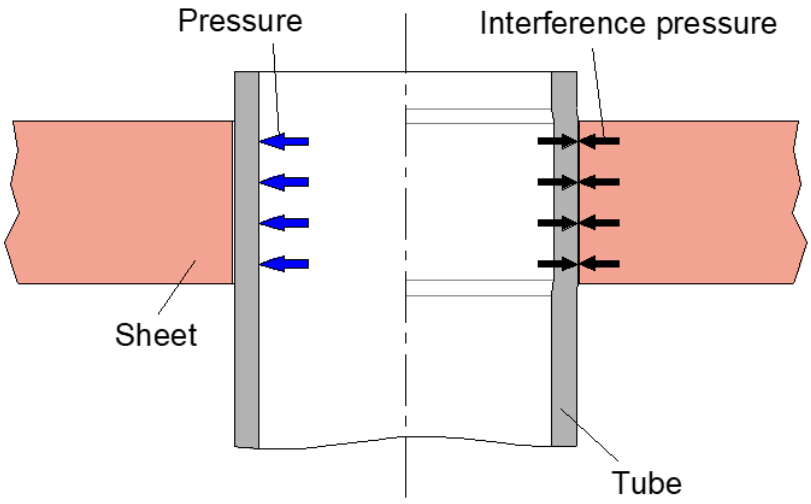

Figure 2.3: Interfacial Pressure Joining.

2.2.2 Mechanical Interlocking Techniques

The sheet-tube connections that base its nature on mechanical interlocking mechanisms are those that combine both plastic flow and utilization of different features such as bends, curls, dimples and cut-outs, to provide a specific shape and enforce a connection between the joined components.

In the work of Altan et al. [7], the mechanical interlock could be obtained expanding the tube and forcing the clinching mechanism with the sheet. Some other featured techniques expanded the tube through flexible rubber plugs, pressurized fluids or electromagnetic pressure, creating joints anywhere along the tube, as can be seen in Figure 2.4.

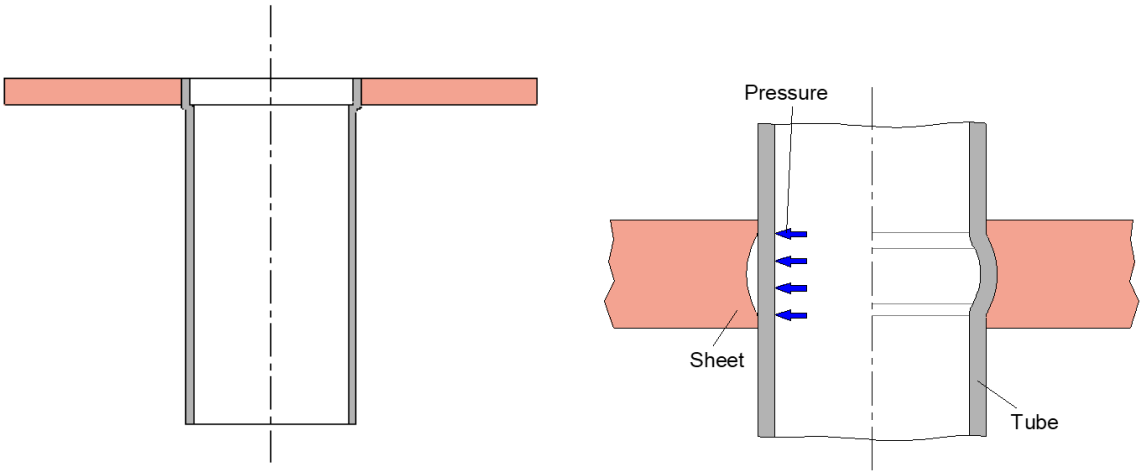

(a) Sheet-tube joint obtained.

(b) Detail of the mechanism.

Figure 2.4: Mechanical interlocking techniques by tube expansion.

Another technology used for creating joints based on a mechanical interlock looked at the development of instability waves in order to provide shape and support for sheets or other components to be joined being designated as both Joining by Upset Bulging or Compressive Beading. Early publications by Lange et al. [8] and Spur et al. [9] look at the creation of these beads, without really focusing on practical applications. It was then, in a patent published by BMW [10], that an application that aimed to join tubes to sheets using this technique was studied. In this patent it was shown that is was possible to join these components using a single stroke risking, however, the creation of unsymmetrical due to material inhomogeneity or incompatible boundary conditions in the process, compromising the overall quality of the joints created. Another problem with this technique is related to the fact that it can't be successfully applied to materials with a low fracture toughness as a significant tension stress field appears in the bead's core, resulting in cracks that propagate throughout the formed tube bead.

A way to avoid crack nucleation and propagation was later studied by Sizova et al. [11] and aimed at creating compression beads with an angular input in order to ensure a more compressive stress field that could avoid the nucleation of a crack. The advances in the technology end up limiting the applicability of this technology as the beads are oddly shaped and difficult practical applications.

The big advantage of this joining technology is the possibility of joining sheets to tubes away from the tube's end, thus providing a flexibility in terms of materials and geometries that can be produced.

It's important to note that the development of beads on the tubes not only serve as a support for the sheets to which will be joined but they can be also used to perform the interlock between the sheet and tube. Other techniques can be used such as flaring or tube inversion in order to create a flap that would substitute the second compression bead.

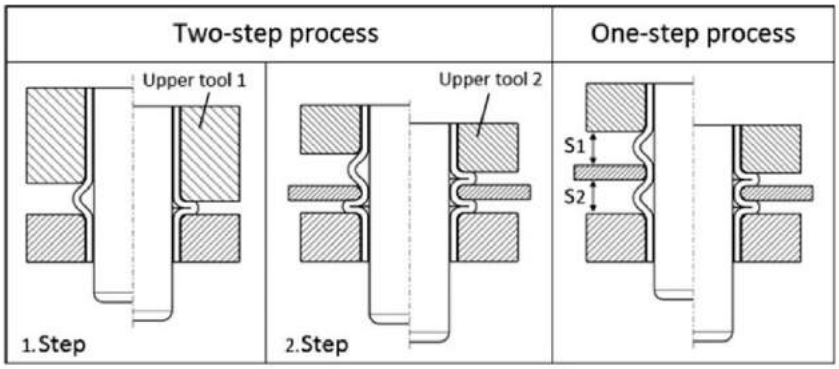

(a) Double Compression Techniques (One and Two Step Processes) (Sizova, 2017)

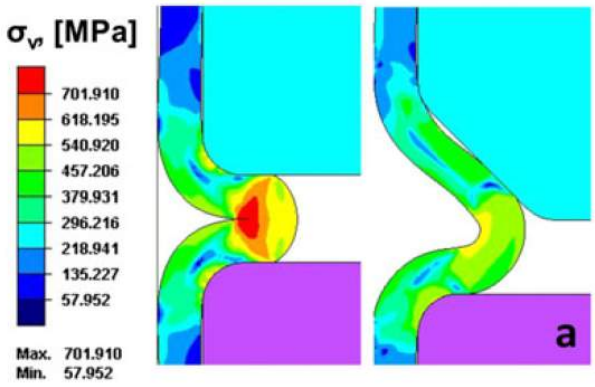

(b) Angular modification to upper die to avoid crack nucleation and propagation (Sizova, 2017).

Figure 2.5: Experimental and Numerical Results

Flaring operations base its nature on the works performed by Reddy [12], Rosa et al. [13–15] and Sekhon [16] in operations designated as External or Internal tube inversion and proved to be a cheap and quick solution that allowed further research and efforts to promote new joining by forming techniques. An intensive study was made in order to define the main parameters that would allow the inversion to occur successfully, as it must be noted that a tangential and radial expansion occurs in the tube and it inverts. The main parameter found was the curvature radius of the inverting matrix, as it held major responsibility for the extension and stress fields created.

Transposing the theoretical and experimental knowledge from this tube inverting technology, Alves et al. [2] published, in 2011, an article that incorporated both compression beading on tubes and flaring through tube inversion. In the same paper, an interesting application was presented that involve the combination of the previous operations to produce a seat-back bottom frame used on cars and trains,

in-between others. The authors also concluded that the developed joints end up performing better when compared to the welded joints for the same structure and the main disadvantage was the two operations that it required.

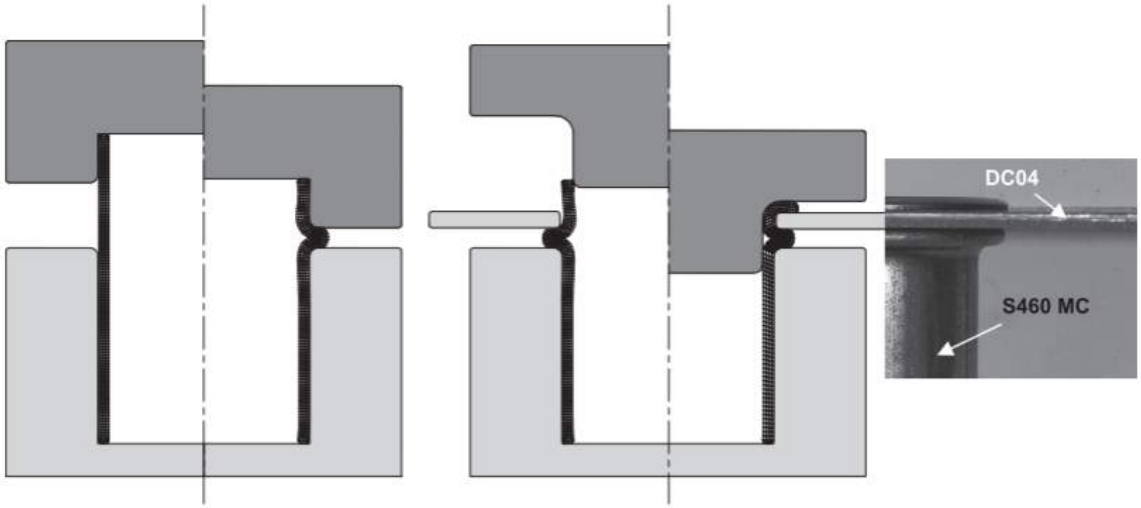

Figure 2.6: Finite element meshes of the first operation to produce the tube bead (on the left) and a second flaring operation to joint the two components as well as an example of the resulting joint using two different materials (on the right). (Alves et al., 2011).

In 2013, Alves et al. [17] were successful in creating a joint that was capable of performing the same joint in a single operation. The following figure presents the setup that was used to join the sheet to the tube where the upper die compresses the tube against the lower flaring die and finally due to the gap between the two dies, a instability forms in the tube, forming the bead that supports the sheet.

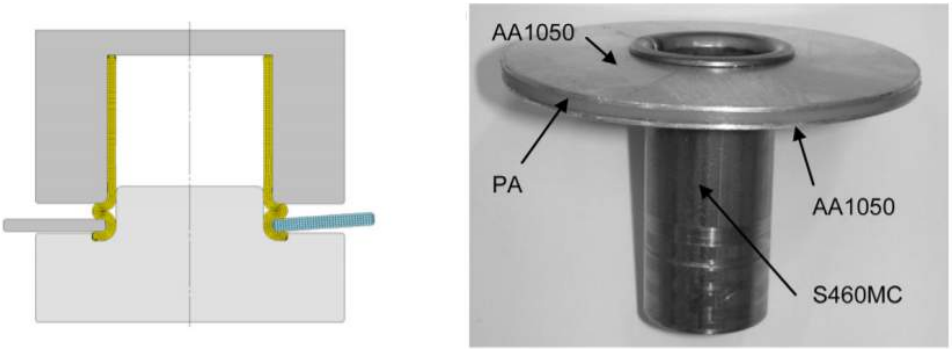

Figure 2.7: Setup used for performing the sheet-tube joint in a single stroke with the mesh used (left) and a photograph of the resulting joint. (Alves et al., 2013).

Further developments were made to this technology with applications on inclined planes as shown in the following figure. [18] and Gonçalves et al. [19].

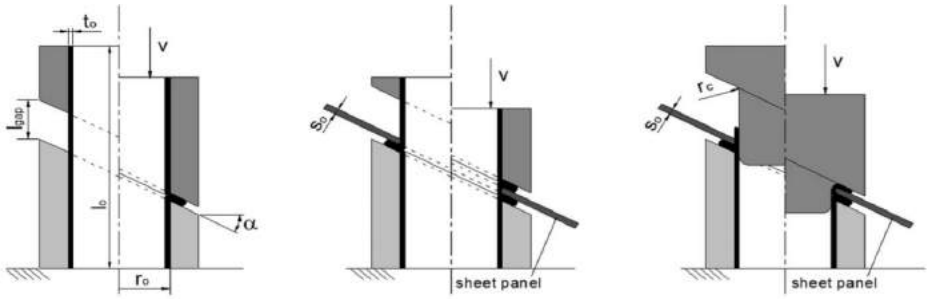

(a) Joining by forming through Double Compression Beading and through Flaring (Gonçalves et al. 2013)

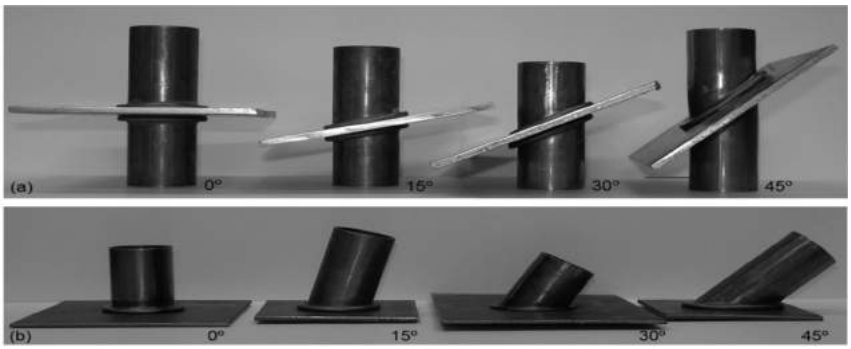

(b) Experimental results for joining in inclined planes (Gonçalves et al., 2013).

Figure 2.8: Joining by Forming in Inclined Planes through combination of Compression Beading and Flaring operations.

In recent years, a lot of research has been carried out in yet another technique to assure tube to sheet connections through mechanical interlocking based joints. In particular, Alves et al. [20], revealed a new technique that based it's mechanism on the early papers by Sieczkarek et al. [21] and Merklein et al. [22, 23] and aimed to replace and solve the setbacks of compression beading on tubes. This technology was designated as sheet-bulk forming which consisted in a partial compression of the tube's thickness. The piled-up material will work as a support to place a sheet and after a secondary operation to lock both the sheet and the tube, a joint is then produced as is shown below in Figure 4.2.

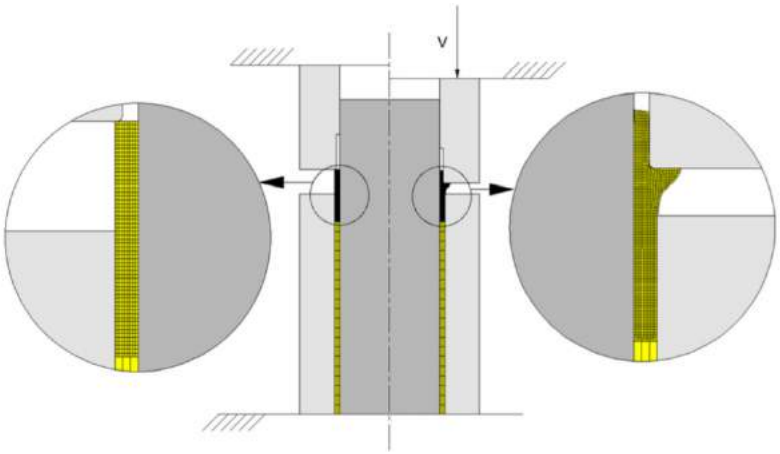

Figure 2.9: Finite Element scheme of the Sheet-Bulk Compression of tubes. (Alves et al., 2017)

However, this operation revealed some problems related with crack opening on the sheet-bulk formed flanges. Alves et al. [20] thoroughly studied the parameters and concluded that in order to obtain sound flanges, a compromise solution between the fraction of the sheet thickness that was compressed and the height of the gap (that would determine the size of the flange) had to be found, or else some crack opening on the sheet-bulk formed flanges may develop. In fact, the limited amount of material that could be piled-up were the drawbacks that ended up limiting this process' applicability and performance.

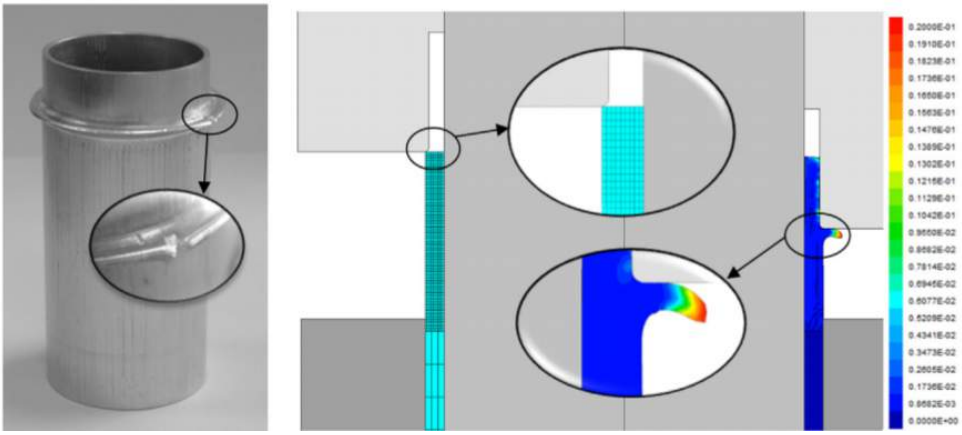

Figure 2.10: Sheet-bulk forming on tubes with a detail of the development of cracks on the flange for incorrect process parameters. (Alves et al., 2017).

Nevertheless, it was proved by the authors in question that this could be presented as yet another solution for joining sheets to tubes that could replace the conventional techniques that were already discussed.

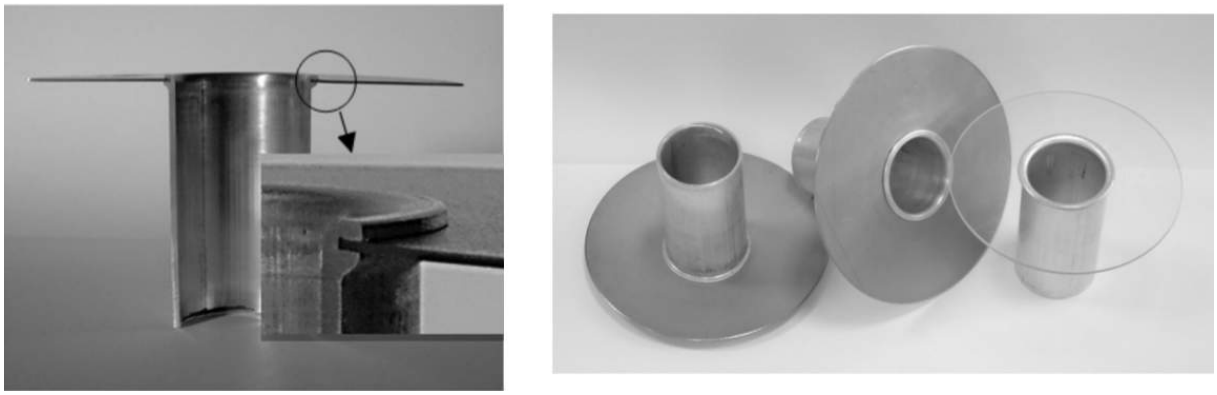

Figure 2.11: Experimental results for sheet-bulk forming of tubes and the joining with sheets after a secondary locking operation. (Alves et al., 2017).

As an evolution of the previous sheet-bulk forming process, Alves et al. [24] published, in 2017, a paper that looked at the creation of annular flanges in a different way than had been done before. The reconfiguration of the previously used die allowed to constrain the outward flow and therefore, avoid the cracking at the free surface and allowing to customize the size and shape of the annular flange. This process was designated as Boss forming and in Figure 2.12, a schematic picture showing the two processes (Sheet-Bulk Forming and Boss Forming) allows to differentiate the techniques.

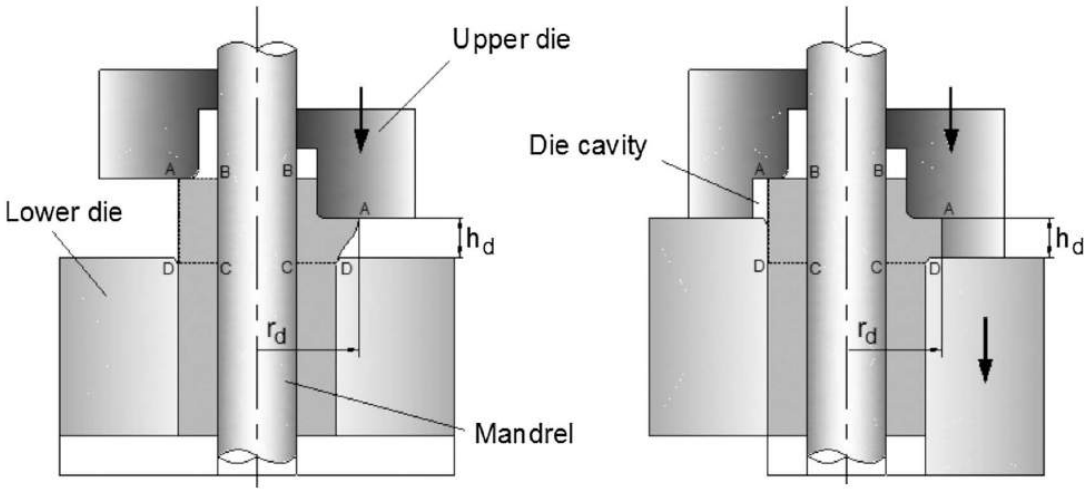

Figure 2.12: Comparison of Sheet-Bulk Tube Forming and Boss Forming (Alves et al., 2017).

Alves et al. [24] concluded in the paper that in fact this modification to the process of fabrication of annular flanges is a clear improvement, as a larger amount of material can be piled-up with this process, which allows a better performance of joints fabricated using this technique (as will be further seen). However, cracking of the annular flanges or buckling during the pile-up process can still happen if improper use of the main parameters is verified. The authors defined three modes of deformation that may be verified: Mode I corresponds to sound annular flanges whereas Modes II and III correspond to buckling and cracking in the formed annular flanges, respectively. whereas Modes II and III represented buckling and cracking, respectively.

Buckling occurred for cases where the values of the height of the die cavity for parameter h_d (represented in Figure 2.12) were too large, as for cracking it occurred in the free surface when the values of the width of the die cavity w_d. This allows to conclude that the success of the operation depends on these two main parameters and a compromise solution between both had to be found in order to obtain sound annular flanges.

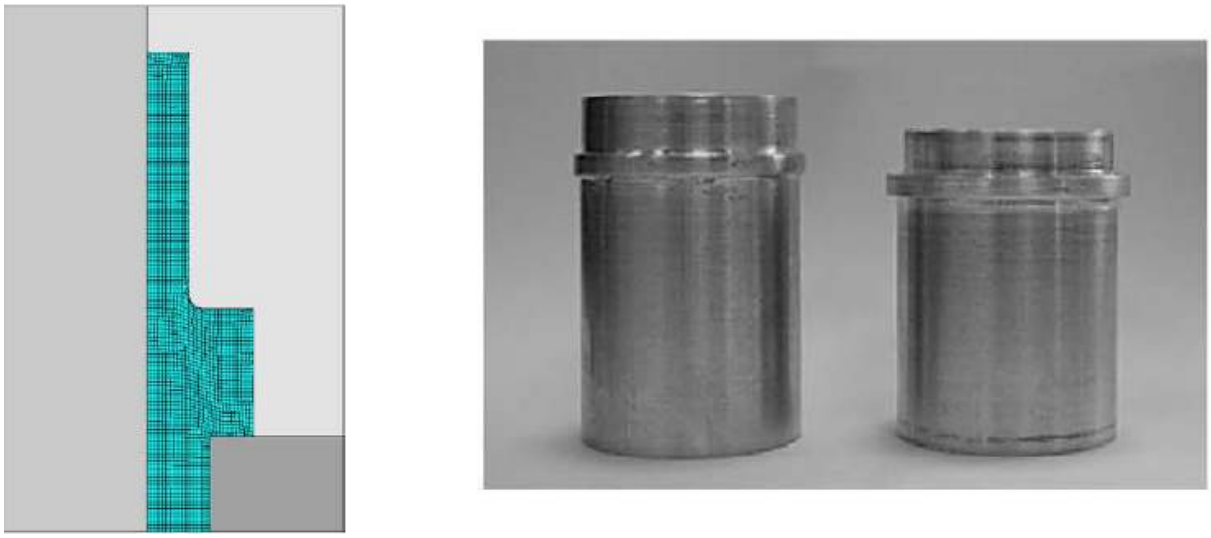

Figure 2.13: Finite Element mesh of Annular Flange and experimental results (Alves et al., 2017).

The development of the boss forming process was made trough the combination of this technology with other joining technologies as mentioned in the previous sections, to develop sheet-tube joints in-between other combination of geometries and led to various articles that presented these new solutions [25–27].

3

Experimental Development

Contents

In this chapter, the experimental development of the thesis will be discussed. The presented topics will regard the types of experimental test performed, their respective procedures and the variables they included. The experimental tests performed covered the progress from material flow curve determination, to the determination of the force needed to form a new surface as the squeezing punch progresses trough the sheet thickness during the joining by forming process. Experimental tests with the standalone sheet with an inner hole tests to understand the influence of the tube in the overall joining process were also performed, among others. Finally, an explanation will be given on how a joint performance was measured, to validate the produced sheet-tube joint.

3.1 Process description

The joining of tubes to sheets was obtained by a cold forming operation done at room temperature and consisted in squeezing the adjacent region of a sheet with thickness t_s in order to promote a flow of material from the sheet towards a tube with a thickness t_0 and an inner radius r_0. An inner tube bead was hereby formed assuring the mechanical interlocking between both these components.

This process is conducted by a specifically designed tool, that will hereafter be designated as the squeezing punch and develops itself in a single stroke operation. The tool is tubular and has a rectangular *l x h* cross-section recess, where *l* and *h* are the length and height, respectively. The sheet is supported by the lower die in order to prevent the sheet from moving downwards and an axial squeezing force is then applied by the squeezing punch, while keeping the lower die immobile. The operation is carried out to a predefined depth so that to shape the inner tube bead.

Note that the fact of one die being stationary will promote (and further discussed later) a highly asymmetrical deformation. The asymmetry of the deformation will greatly affect the quality of the joint obtained and for that reason it had to be thoroughly studied in order to optimize the process' parameters. It was then possible to study the relationship between the various parameters and combine them in order to obtain sound joints, however the flat surface of the lower die supports the sheet and prevents its tilting or misalignment during indentation by the upper die. This is the main reason why the process was not designed symmetric. Of course, the process could be designed symmetric, as it is shown on the right hand side of the schematic drawing included below, where springs or the elastomers would prevent tilting and misalignment but the overall process would require a double acting force for the resulting joint to be symmetric. This requirement is more difficult to ensure in applications performed on site and this was the main reason for designing the process as it is shown on top schematic drawing.

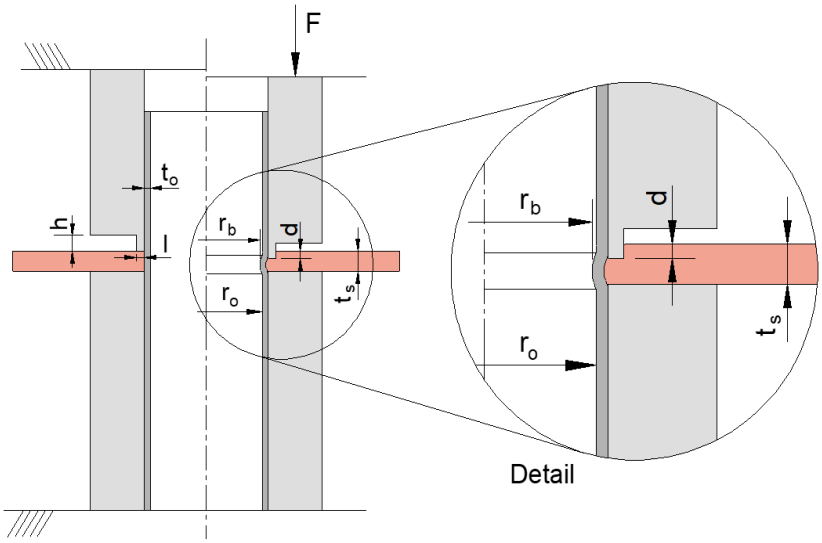

(a) Schematic representation of the tool system utilized for joining sheets to tubes by annular sheet squeezing, at the open and close positions.

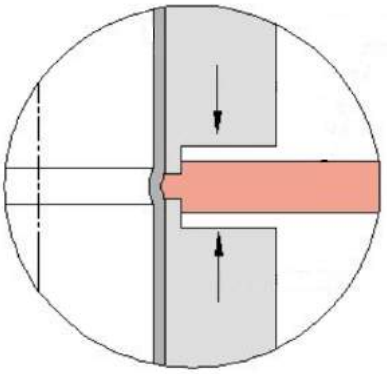

(b) Mechanical Joint final result.

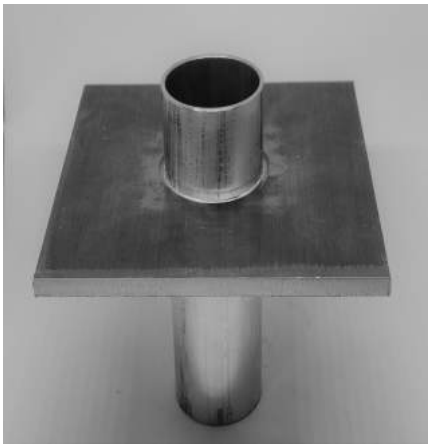

(c) Mechanical Joint final result.

Figure 3.1: Process Description

The variety of materials that can be successfully used is one of the big advantages of the process. The only limitation regarding this topic is exposed when the material of the tube has a much higher strength than the one of the sheet. This situation would cause the materialto flow outwards and not against the tube and therefore not creating the inner tube bead needed to lock the two components, leading to an unsucessful joint.

The result will be a uniform sheet-tube connection where one of the surfaces of the sheet shows the squeezing marks that promote the flow of material while the other surface remains untouched. This connection is permanent unless a sufficient load is applied to destroy the mechanical interlocking.

3.2 Material Characterization

3.2.1 Elastic Compensation

Before any experimentation, it's essential to understand that in any experimental test, the loads applied will cause elastic deformation to both the component and the test machine, in this case the hydraulic testing machine. Hooke's law allows to conclude that any load will cause a deformation. Because of this, it becomes necessary to model a compensation curve to make sure the results obtained refer only to the components tested and don't include the additional deformations of the system.

It was then possible to identify two distinct behaviours of the curve. For values of displacement below 200 mm, the curve could be accurately fitted by a 3rd degree polynomial function, as for values of displacement (x) superior to 200 mm, the curve could be fitted by a simple linear equation.

$$x_c = \begin{cases} 0.00012x^3 - 0.00009x^2 + 0.00590x + 0.00362 & \text{if } x < 200 \\ 0.0017x + 0.1409 & \text{if } x > 200 \end{cases} \tag{3.1}$$

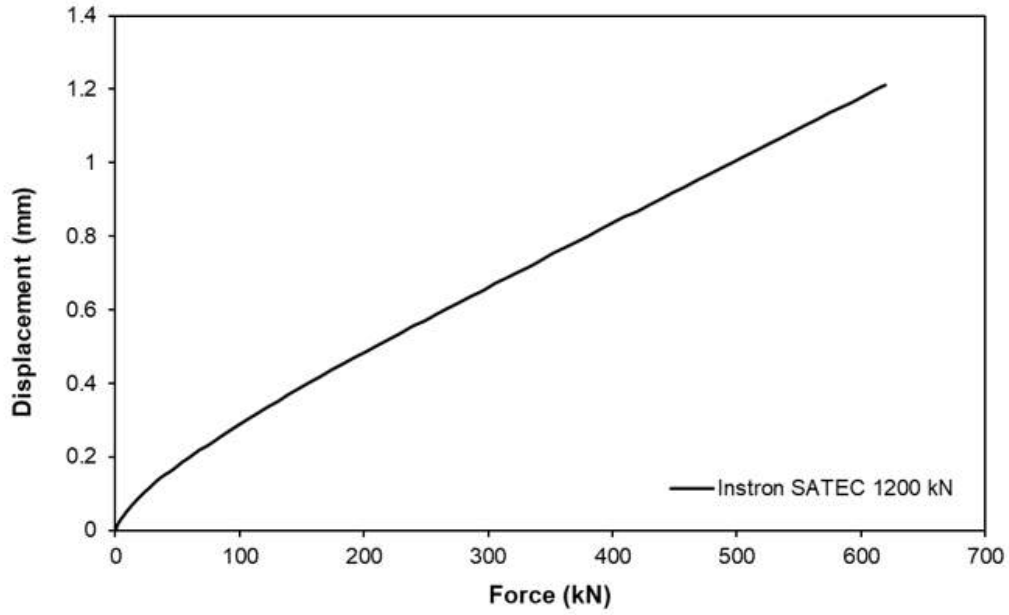

Figure 3.2: Compensation Curve for the Instron SATEC 1200 kN

3.2.2 Flow Curves

The experimental work that led to the development of this new joining by forming process made use of AA5754-H111 aluminium sheets with a 5 mm thickness t_s and AA6063-T6 aluminium tubes with an inner radius r_0 of 14.5 mm and 1.5 mm wall thickness t_0.

The flow curves (true stress - true strain curves) of both materials were determined from tensile and stack compression tests carried out in a hydraulic testing machine (Instron SATEC 1200 kN) with a cross-head speed of 5 mm/min. In both cases, samples were removed from the original sheets and tubes to be used in the experimentation works and machinto a circular/disk shape.

To retrieve the flow curve of the tube's aluminium alloy, the stack compression tests were performed with disks with a 10.4 mm diameter and a total height of 4.28 mm. Similarly, the flow curve of the aluminium sheets was obatined obtained through the compression of disks with a 22.02 mm diameter and a total height of 14.72 mm. The resulting flow curves after merging the experimental data retrieved from the tensile and stack compression tests are shown in Figure 3.3.

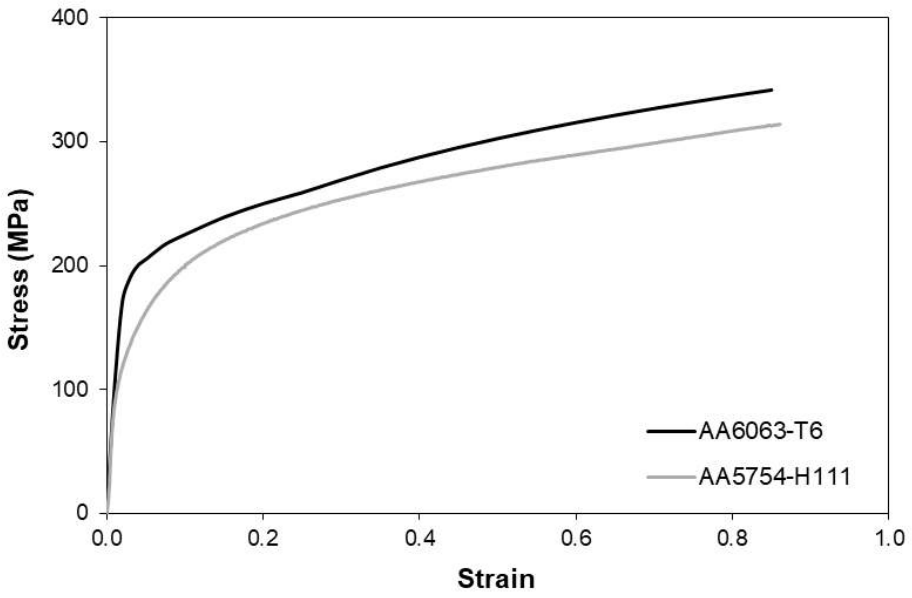

Figure 3.3: Flow Curves of the two aluminium alloys used in the experimental work.

3.3 Equipment, Tools and Preforms

3.3.1 Experimentation Equipment and Preforms

In the development of this new Joining by Forming process, every single operation was operated in the laboratory of Tecnologia Mecânica in Instituto Superior Técnico. For every different study, the same preforms were used.

The aluminum AA6063-T6 tubes were were cutted to a length of approximately 100 mm and the aluminum AA5754-H111 sheets were cutted with dimensions 100 x 100 mm (width x lenght). A diameter hole of 32 mm (corresponding to the external diameter of the tube) was made in those sheets and all tubes and sheets were lubricated with zinc stearate, before being assembly on the tools setup.

3.3.2 Tools

Different tools were fabricated depending for the different tests performed. For the first set of tests, the influence of the cross section recess (*l x h*) on the quality of the joints was studied and for these experiments, the squeezing punch (upper die) was machined in the lathe with a constant dimension for *h*and different values of the parameter l, ranging from 0.5 mm to 5 mm.

When studying the effect of the depth *d* in the quality of the joint, the parameter l was kept constant and the parameter *h* was increased to avoid direct contact of the squeezing punch periphery with the sheet. The dimensions of the lower die were kept constant troughout all tests.

The die used for the destructive pull-out test had a 32 mm diameter hole so the tube could fit and a small clearance made by a counter bored hole on the top of the touching die surface. All dimensions remained constant and all components mentioned in this section. For every set of tests, the geometry of this die was not altered. The components above mentioned can be seen in Figure 3.4.

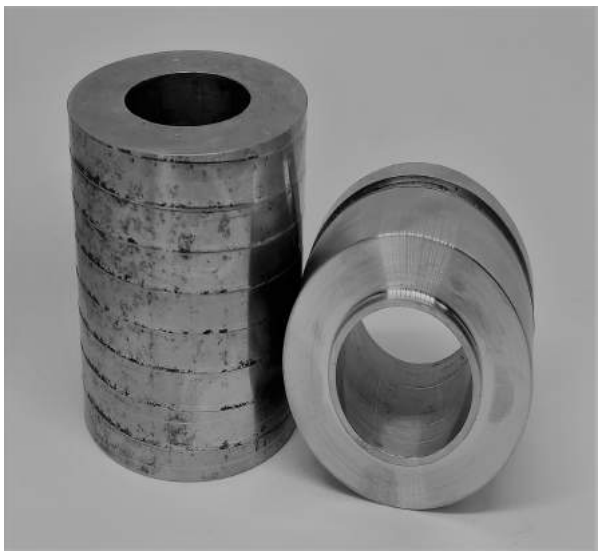

(a) Active components. To the right is the lower die and to the left is the squeezing punch.

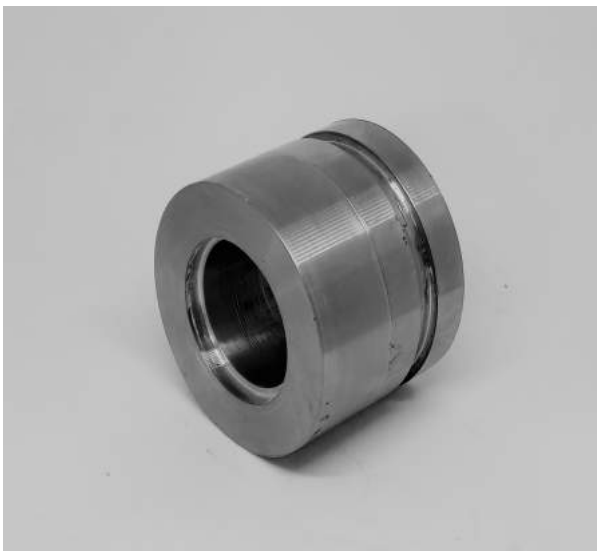

(b) Die for destructive pull-out tests.

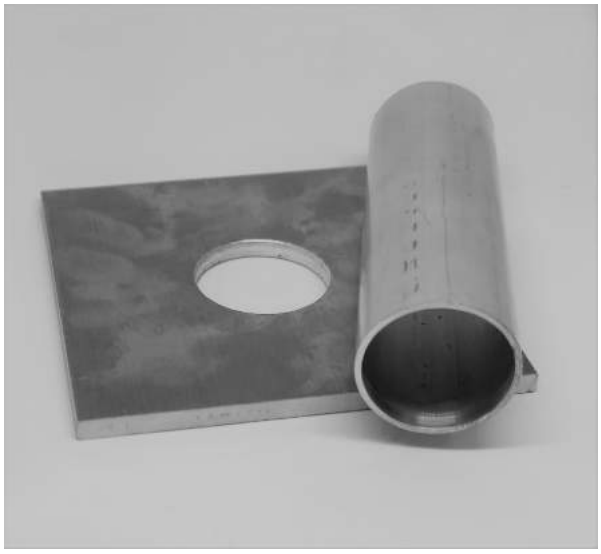

(c) Preforms

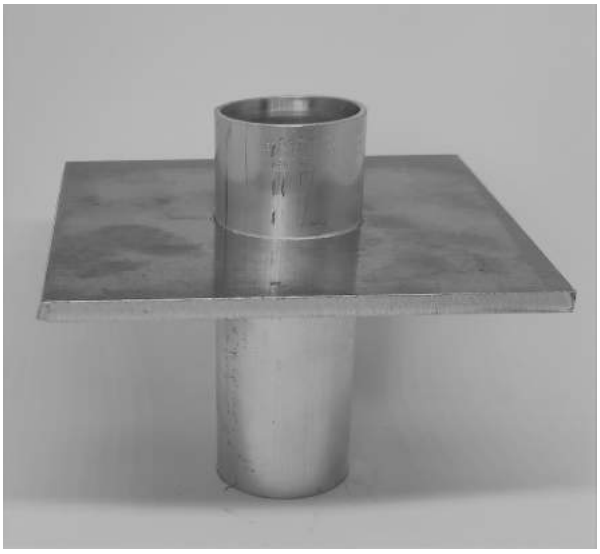

(d) New sheet-tube mechanical joint.

Figure 3.4: Tools and Preforms used in the experimental development.

3.4 Methods and Procedures

The different experimental work plans are based on 4 different types of tests as will be described on the following sections.

3.4.1 Test Type I - Upset Compression of Rings

This type of test consisted of squeezing an AA5754-H111 aluminium ring, whilst in one case, constraining the outer flow of material and in the other, not constraining the flow of material. The objective of this test is to understanding the energy and force inherent to the opening of a new surface that results from material separation at the cross-section recess corner of the squeezing punch along the squeezing depth of the sheet being squeezed. Conclusions can be drawn when comparing this test with the following tests. The work plan for this test and their respective schematics are presented in Table 3.1.

Test Case	r_0 (mm)	t_0 (mm)	t_s (mm)	l (mm)	h (mm)	d (mm)
Upset Compression of Rings without Outward Constraint						
1R	14.5	-	5	1.8	-	2
2R				2		
Upset Compression of Rings with Outward Constraint						
1RC	14.5	-	5	1.8	-	2
2RC				2		2

Table 3.1: Work plan for upset compression of aluminium rings, for the different constraint situations.

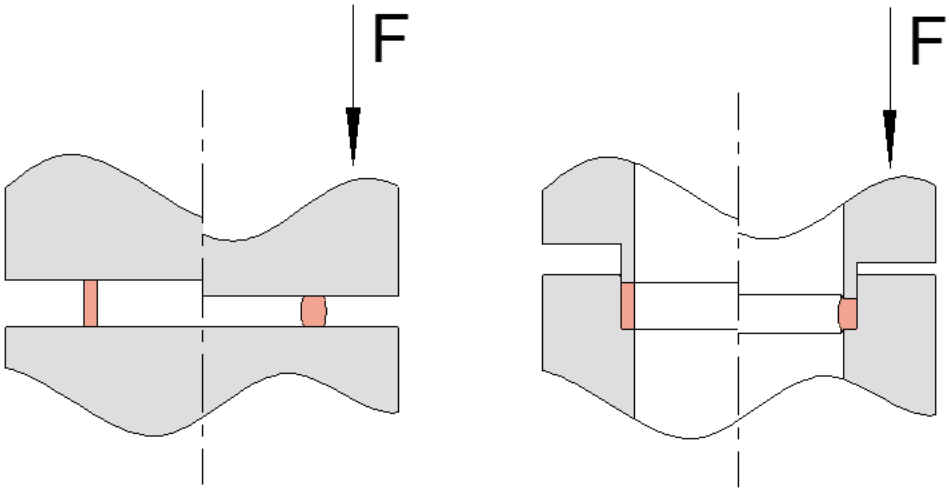

Figure 3.5: Schematic representation of the setup utilized in the upset compression of rings. To the left, without outward contraint and to the right, with outward constraint.

3.4.2 Test Type II - Annular Sheet Squeezing

The Annular Sheet Squeezing was another type of test performed during the experimental development. The test consisted in the local compression of a standalone AA5754-H111 aluminium sheet with an inner hole with a 32 mm diameter (the same sheet that will be used for performing the sheet-tube joints) with a squeezing punch which dimensions are presented in Table 3.2, however, the set was different as the tube wasn't present. The main goals of these experimental tests were to compare the *Force-Displacement* evolution of a standalone sheet versus the sheet and tube set and to understand how relevant the shear stresses were in the formation of new surfaces, as discussed in chapter 3.4.1. The work plan is depicted below in Table 3.2.

Test Case	r_0 (mm)	t_0 (mm)	t_s (mm)	l (mm)	h (mm)	d (mm)
1S	14.5	-	5	1	-	2
2S				1.5		
3S				1.8		
4S				2		

Table 3.2: Work plan for the Annular Sheet Squeezing tests.

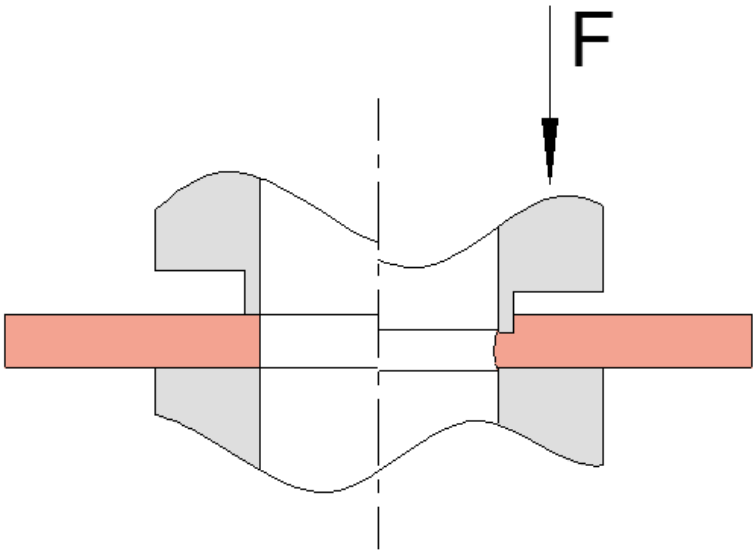

Figure 3.6: Schematic representation of the setup utilized in the annular sheet squeezing tests.

3.4.3 Test Type III - Joining by Forming

In this section, it's important to refer that two distinct experimental work plans were built. Firstly,(adicionar referência?) the influence of the cross-section recess length *l* was being studied. The tests were carried out exactly as depicted in Figure 3.1, applied to the tube and sheet setup.

The overall investigation on the new joining by forming process allowed the identification of the following main operating parameters: (i) the sheet and tube materials to be joined, (ii) the tube inner radius, (iii) the tube wall thickness, (iv) the sheet thickness, (v) the cross-section recess length and the (vi) squeezing depth.

The geometry of the tube, aswell as that of the sheet, were kept constant throughout the whole process. The only parameter that suffered change was the cross-section recess length *l*, as its influence was the highlight of study at this stage. The squeezing depth *d* was kept constant and equal to 2 mm. This allowed to have a common reference base to thoroughly compare the reuslts obtained and reach plausible conclusions about the type of flow. However, small variations of the squeezing depth were analyzed with finite element, as will be later be presented. The work plan is presented in Table 3.3.

booktabs multirow graphicx [table,xcdraw]xcolor

Test Case	r_0 (mm)	t_0 (mm)	t_s (mm)	l (mm)	h (mm)	d (mm)
1	14.5	1.5	5	0.5	2	2
2				1		
3				1.5		
4				2		
5				2.5		
6				3		
7				5		

Table 3.3: Work plan for the study of the influence of the cross-section recess length.

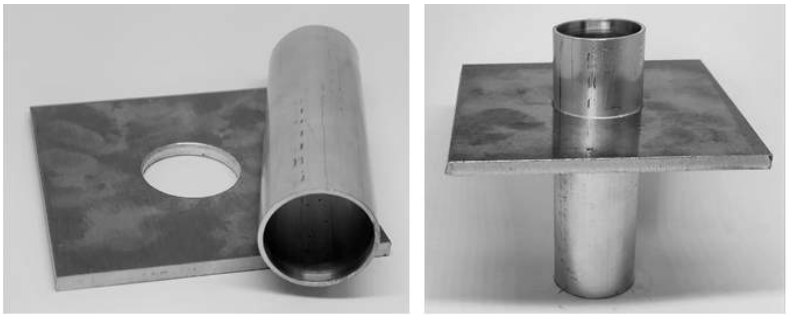

Figure 3.7: Preforms and final result of the Joining by Forming tests.

At a later stage, the influence of the squeezing depth *d* was analyzed. Hence, and as referred above, the tool had to be adapted for the work plan that derived from this study. In contrast to the previous work plan, the cross-section recess length was maintained constant and equal to 2 mm, while the squeezing depth was varied. The goal of this study was to understand the influence of *d* in the size of the inner tube bead and what implication it would have on the destructive pull-out force. However, and similarly to before, small changes were made to the cross-section recess lengths, but only with finite element modelling. The work plan is presented in Table 3.4

Test Case	r_0 (mm)	t_0 (mm)	t_s (mm)	l (mm)	h (mm)	d (mm)
8	14.5	1.5	5	2	4.7	1
9						2
10						3
11						3.5
12						4

Table 3.4: Work plan for the study of the influence of the squeezing depth.

The third work plan regarding the joining by forming tests included the addition of an angular incline to the contact surface of the squeezing punch, as shown in Figure 3.8. The work plan associated with this study defined as main parameters the cross-section recess length *l* and the squeezing depth *d*. The reason behind having to consider the squeezing depth is related to the process' deformation change when an angular incline is added to the contact surface of the tool, which will hereafter be designated as α. The quantity of material that will suffer plastic deformation is smaller than that of the joining by forming test where α is equal to 0º. Therefore, test were made where *l* was maintained constant and different depths and angular inclines were essayed. The work plan is presented in Table 3.5.

Test Case	r_0 (mm)	t_0 (mm)	t_s (mm)	l (mm)	h (mm)	α (º)	d (mm)
13	14.5	1.5	5	2	4.7	15	2
14							2.5
15							3
16						30	2
17							3

Table 3.5: Work plan for the study of the influence of the angular incline in the contact surface of the squeezing punch.

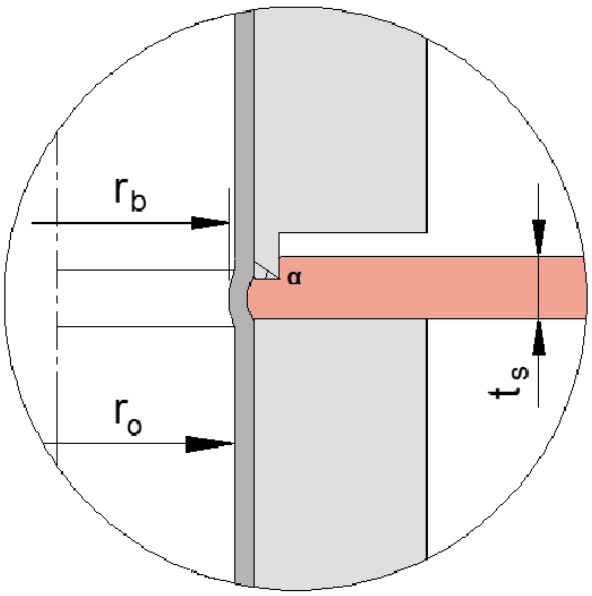

Figure 3.8: Schematic representation of the Contact Surface angular incline.

3.4.4 Test Type IV - Destructive Pull-Out Tests

This type of experimental tests consisted in destructive pull-out tests to evaluate the maximum force that the new sheet-tube joints are capable to withstand before failing. There are two types of setup used for this test. Those are shown in Figure 3.9

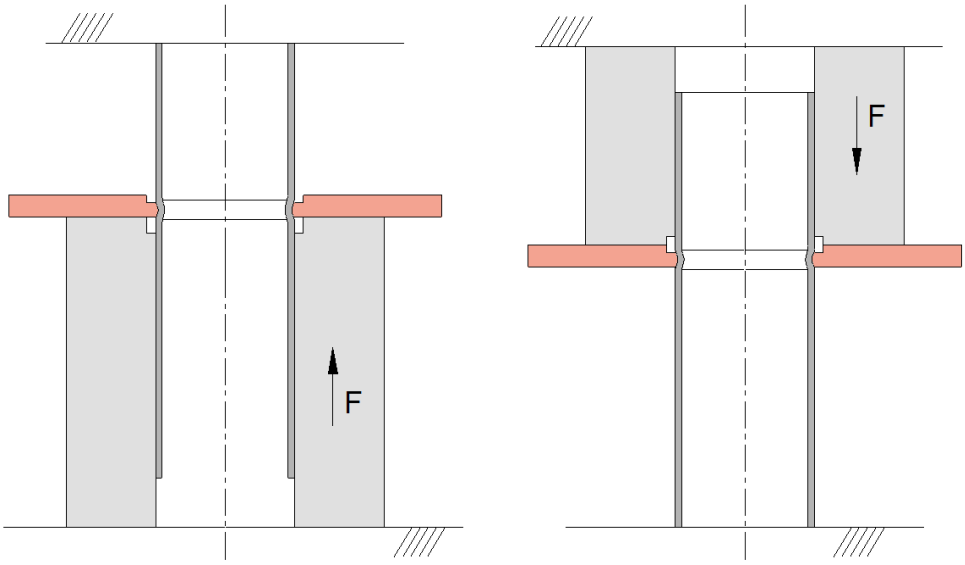

Figure 3.9: Schematic representation of the setup utilized in the destructive pull-out tests. The arrows show the two different pulling-out directions.

4

Finite Element Modelling

Contents

In this chapter, the finite element development will be discussed. Numerical simulation using the Finite Element Method (FEM) is essential to any project as it provides reliable results about the outcome of any process before any experimental work is even necessary. A deeper knowledge of the process can be obtained from analyzing FEM results as the information provided from the numerical simulations allows conclusions about the stress and strain fields in every element of the created mesh as well as other process variables. Another advantage of the numerical analysis is the determination of critical deformation regions, that can lead to optimized solutions and improvements to the global process.

The presented topics will show all the different numerical simulations performed, and the main parameters that were put under scope during the numerical development.. As referred in the previous chapter, for every Joining by Forming experimental test that was performed, small variations of the main parameters were modelled into the finite element software I-form2d that was utilized. Those variations will be presented in this chapter and the results that derived from those will be later presented.

Some examples of FEM simulations that were performed go from the upset compression of rings to the different parameters tested for the new developed joining by forming process. Some simulations were also made with some other geometrical variations to the squeezing punch, such as the addition of angular inclines to both the lateral and contact face of the tool. The pull-out destructive tests in both directions were also simulated trough the numerical software.

4.1 Mesh Creation and Refinement

The I-FORM2D software was used to create and refine the meshes of both the sheet and the tube. The degree to which a mesh is refined demands a compromise to obtain the best results without long simulation times. A very refined mesh will require much more computing power and longer simulation times as it operates on much more complex matrix systems despite providing better and more accurate results. A mesh that doesn't suffer such a refinement will of course require much less computing power and have results available in a shorter period. Those results may be however, not as accurate as with meshes more refined.

4.2 Process Parameters and Finite Element Model

Through the I-FORM2D Pre-Processor software, it's possible to construct the mesh and define the process' main parameters. In this section, the initial mesh for Case 4 will be shown as it is the main study study case for reasons that will be explained in further sections.

In terms of the definition of the main simulation parameters, one that particulary stands out due to its importance is the *Increment of time between steps*. The importance of this parameter relates to the accuracy of the simulation: The smaller the increment, the more accurate the simulation will be, although implying a longer simulation time. For every simulation, the time increment chosen between steps had a value of 0.01 s and the number of steps varied according to the squeezing depth desired for the simulation.

The dies were defined as rigid objects with a 1 mm/s velocity and a friction factor of 0.1. The reason behind this value relates to the lubrication provided to every die before any experimental test. The friction factor between materials (AA5754-H111 aluminium sheets and AA6063-T6 aluminium tubes) was defined as 0.5. Both friction factors result from checking the value that best matched the experimental results.

After having the simulation's main controls, iteration and dies parameters well defined, friction and contact parameters ought to be thoroughly defined. In order to accurately simulate the experimental simulate the experimental conditions during the plastic deformation, the contact between nodes was defined with the option of releasing themselves from each other during the simulation.

The tube was discretized with around 800 quadrilateral elements and the sheet had approximately 20000 quadrilateral elements before remesh operations were performed. A local refinement was made to the region of the sheet that was to be subjected to deformation, allowing for more precise results while not requiring for too much computing power and simulation time.

The initial and final mesh for Case 4 are shown in Figure 4.1 where it is possible to observe the local mesh refinements made to both the sheet and the tube. In the second figure of the final result of the simulation, it's possible to observe the overall refinement that was done during the intermediary remesh operations. The simulations took between 60 and 100 minutes to be completed and this simulation time depended on the number of steps that were needed (higher number of steps for deep squeezing depths).

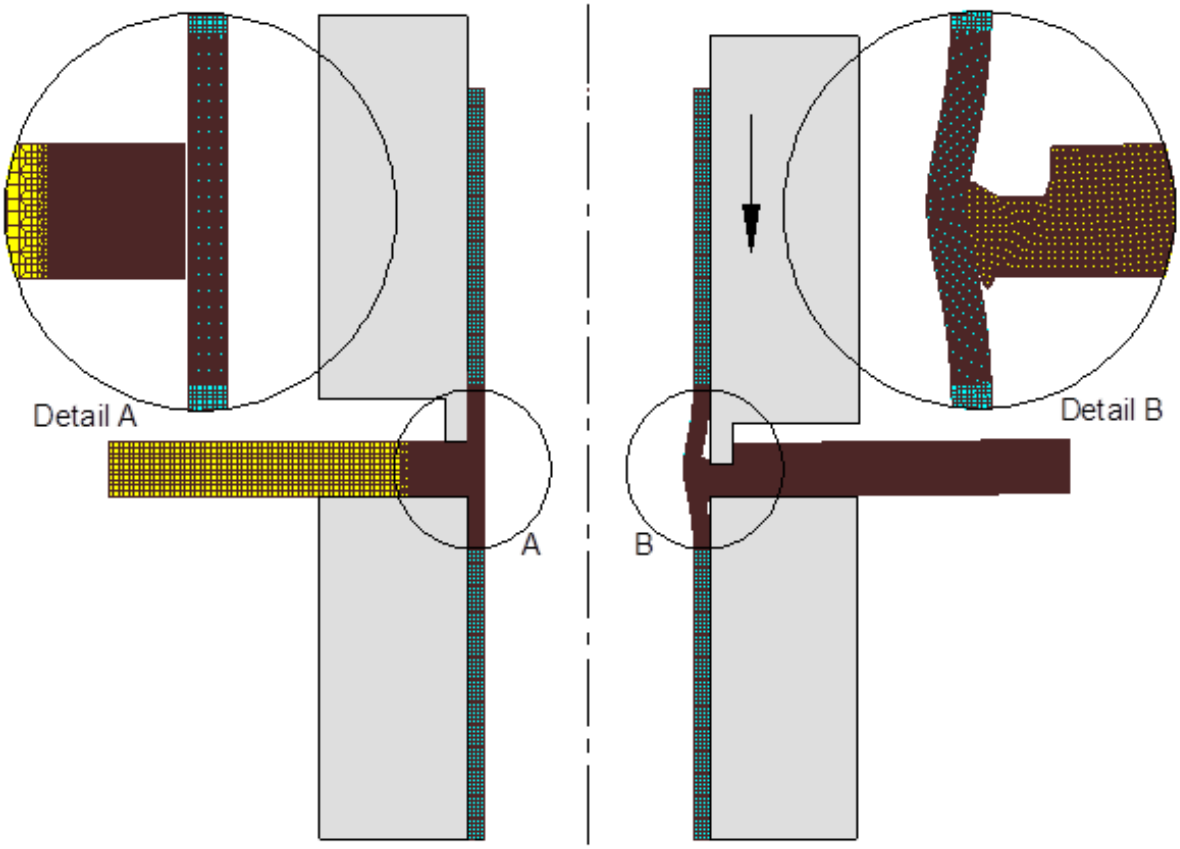

Figure 4.1: Initial and Final FEM model for Case 4.

4.3 FEM Work Plan

In this section, the various simulations effectuated will be exposed and further explained. The main studies that were numerically carried out tried to provide comparative information to the Joining by Forming tests done experimentally and for that reason the simulations that refer to an experimental test aren't shown in this section. However, after the optimization of parameters, the possibility for additional investigation done solely in the numerical software opens as there is a guarantee that the reality is being accurately simulated. Because of that, studies were made that included geometrical changes to the dies such as, inclinations on the lateral face of the squeezing punch and the increase of the tool's inner radius, translated numerically with an increase of the tool's offset with the axis, as will be further shown.

4.3.1 Tool's Inner Radius and Lateral Face Angular Variations Numerical Study

As was introduced in the beginning of this section, some additional studies were made including further investigation regarding the variation of the inner tube radius aimed to understand what the impact would be of starting the indentation further away from the axis than the original simulation and experimental test. The initial hypothesis was that the increase of the inner tube radius would lead to the flow of an entire rigid body instead of only the material in close contact with the tube, leading in posterity to an increase of the inner tube's bead and consequently the destructive pull-out load. The simulations regarding this topic were made by means of an offset. The offset measures the increase of the squeezing punch's inner radius while maintaining the squeezing depth and the cross-section recess length constant and equal to 2 mm. The work plan related to the offset numerical study is presented below in Table 4.1. Note that these test sets were not carried out experimentally and their accuracy are guaranteed from the previous parameter optimization.

t_0 (mm)	t_s (mm)	t_i (s)	f_d	f_m	l (mm)	Offset (mm)	d (mm)
1.5	5	0.01	0.1	0.5	2	0.2	2
						0.3	
						0.5	
						1	

Table 4.1: Work plan for the simulations regarding the influence of the tool inner radius by means of an Offset.

Similarly, the study related to the addition of an angular incline to the squeezing punch's recess lateral face aimed to preview the different way that the sheet's deformation would occur. These differences might include the fact that more material was being guided towards the tube. Increasing the flow of material would increase the inner tube's bead, hence, mechanical joints could withstand superior destructive pull-out loads. The lateral face incline's angle was defined as ϕ. The work plan consisted of maintaining the cross-section recess length and the squeezing depth constant, as done in the previous study, while varying the offset dimension as shown below.

t_0 (mm)	t_s (mm)	t_i (s)	f_d	f_m	l (mm)	ϕ (º)	d (mm)
1.5	5	0.01	0.1	0.5	2	8	2
						10	
						15	

Table 4.2: Work plan for the simulations regarding the influence of the angular inclinations on the lateral surface (ϕ).

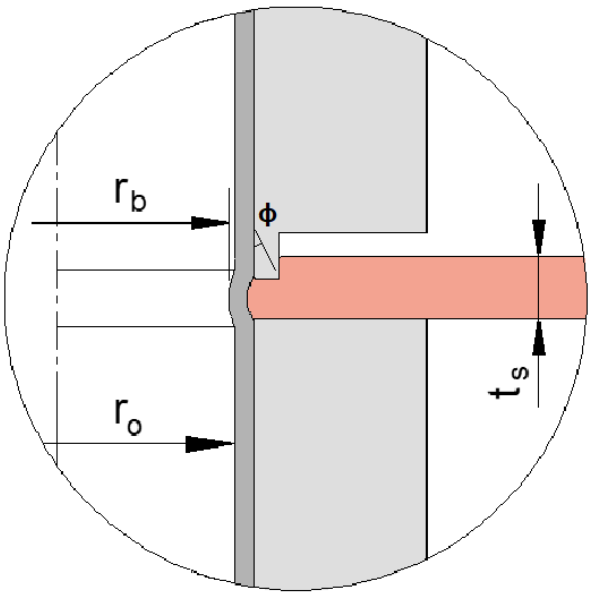

Figure 4.2: Schematic representation of the Lateral Surface angular incline.

4.3.2 Inner Tube's Bead Stationary Behaviour and Sheet Bending Study

Other questions and hypothesis arose throughout the development of the joining by forming process, specially when the squeezing depth parameter was further analyzed and ,as will be seen and further discussed in the next chapter, a linear relation was obtained for the growth of the inner tube's bead when the squeezing depth was increased. Knowing this, a hypothesis emerged that stated that from a critical value of *d* the inner tube's bead dimension might remain constant, independently of any increase of the squeezing depth, leading to a simulation that was made where the sheet's thickness t_s was increased to 15 mm, instead of the original 5 mm and the squeezing depth was set to 11 mm. This simulation would allow the conclusion that for a certain value of the squeezing depth, the inner tube's bead kept (or not) the same dimension and therefore reached a state that was designated as stationary, which gave the study its name.

Another important characteristic of the process that was verified of the process throughout experimental and numerical development was the sheet's bending behaviour as both the cross-section recess length and squeezing depth were increased as the sheet's bending strongly related with the mode of deformation that were obtained and it's nominal length. The different deformation modes were described by Alves et al. [28] by means of a deformation-zone parameter $\Delta = t_s / l$ that allowed to distinguish the so

called deformations modes. Those allowed conclusions regarding the type of flow that was obtained that lead to acceptable or unacceptable joints and the extent to which the sheet would bend throughout the process. Those distinct deformation modes will be thoroughly discussed in the next chapter. In this numerical development, the main study parameter was the sheet length, that will hereafter be designated as s_L The numerical work plan associated with the understanding of these two process characteristics is depicted below in Table 4.3.

t_0 (mm)	t_s (mm)	t_i (s)	f_d	f_m	l (mm)	s_L (mm)	d (mm)
Sheet Bending Behaviour							
1.5	5	0.01	0.1	0.5	2	200	2
						300	
						600	
Inner Tube's Bead Stationary Behaviour							
1.5	15	0.01	0.1	0.5	2	300	13.5

Table 4.3: Work plan for the simulations regarding the Sheet Bending and Inner Tube Bead's Stationary behaviours.

Typical computing time varied from 1 hour and 30 minutes to 3 hours, depending on squeezing depth and whether it was a joining by forming or destructive pull.out simulation. Destructive pull-out simulations tended to take longer as the number of steps was large.

5

Results and Discussion

Contents

In this chapter, the results obtained from both experimental and numerical developments will be presented and discussed. It is the aim of this chapter to gain a detailed perspective of the developed joining by forming technology through the experimental and numerical tests that were made with the specific purpose of finding relations between the parameters previously mentioned as well as other conclusions that may arise from this analysis.

This section will start with the discussion related to the mechanism of formation of new surfaces. The study behind the physics of this mechanism aimed to understand the importance of the shear component of the deformation and quantify it's contribution in the process' required force and energy. The better understanding led to the conclusion that the shear component of the force needed to create a new surface can be neglected and with this, the process' general characteristics were defined and an optimization of the specific parameters shown in Figure 3.1 could be studied.

The influence of the cross-section recess length will then be discussed and it will be defined by means of a deformation-zone parameter, allowing to identify a threshold for this parameter that allows a distinction between sound and unacceptable joints. Following this discussion, the influence of the squeezing depth will be made and its effect on the inner tube's bead dimension is the main aspect of this discussion.

Interestingly, and as will be further explained, it was found that both parameters *l* and *d* aren't independent from each other as it was found that as the squeezing depth increases, the optimal cross-section recess length varies because of a change of the deformation's neutral region position, as shown by numerical plots of the horizontal component of the flow's velocity that allow that conclusion.

Subsequently, the effect of the tool's inner radius variation (numerically modeled with an offset), its lateral surface incline angle (ϕ) and contact surface incline (α) will be presented and discussed. Note that these two parameter alterations aimed to confirm the initial hypothesis that their existence would lead to an increase of the inner tube's bead. The increase of the tool's inner radius would lead to the flow of an entire rigid body against the tube instead of only the material in close contact with the tube. The creation of an angular incline on the tool's lateral and / or contact surface would increase the flow guided towards the tube.

Afterwards, the study regarding the observed bending behaviour of the aluminium sheets throughout the process will be exposed and discussed. The initial hypothesis stated that there would be an optimal sheet length s_L from which the bending would only occur locally instead of occurring in the entire sheet. However, the results contradicted the hypothesis in the sense that a different behaviour was verified showing that the bending does cease to happen, but never becomes a local feature of the process. Additionally, the process' apparent stationary behaviour will be further looked into.

Because this process only bases itself of the flow promoted by an immutable squeezing punch, it was believed that a stationary behaviour would be attained when a certain squeezing depth *d* was verified.

In other words, the inner tube radius would become constant from the moment a certain depth was reached. This would imply that for thicker sheets, there would exist a maximum value for the squeezing depth from which the benefit taken from it, this is, the decrease of the inner tube radius, could not be further improved. This occurs after it was observed that a stationary behaviour can be indeed obtained, but only for very high values of the squeezing depth, assuring the importance of the parameter *d* in the process.

Being the process now fully described and optimized, the forces involved in this process will be scrutinized, in a way that will possibilitate the conclusion on the amount of force or energy that is required to deform the aluminium sheet and the tube.

Finally, the resulting optimal joints will be validated in terms of their performance as the maximum pull-out destructive load for many examples will be shown and discussed, providing further information on the optimal values for the different discussed parameters.

Conclusions will be supported by experimental and numerical data and in the case of the discussion of the new surface formation mechanism, SEM (Scanning Electron Microscopy) observations of a joint's surface were made in order to show the nature of the deformation in specific and well known places.

5.1 Physics of the New Surface Formation Mechanism

In the development of the process, the need to understand the contribution of the shear stresses was of paramount importance to understand the physics behind the formation of a new surface and its effect on the process' forces.

The most important tests and results that needed to be assessed in order to obtain conclusions on this matter were related to fractography imaging on SEM, experimental and numerical force-displacement evolutions comparison between upset ring compression (with and without outward constraint) and annular sheet squeezing and of course numerical results for field variables such as distortion γ and shear stress τ. In particular, the SEM pictures taken were expected show the sheet's surface evidencing the formation of dimples that could instantly accuse shear behaviour. However and as will be seen below, SEM imaging did not allow that conclusion and only experimental and numerical values led to those conclusions.

5.1.1 Fractography Imaging of the Surface

To obtain a deeper knowledge of the very nature of the process, Alves et al. [29] used SEM imaging on the surface obtained in experimental Case 12 and it was possible to distinguish 4 different zones in the surface, as seen in Figure 5.11.

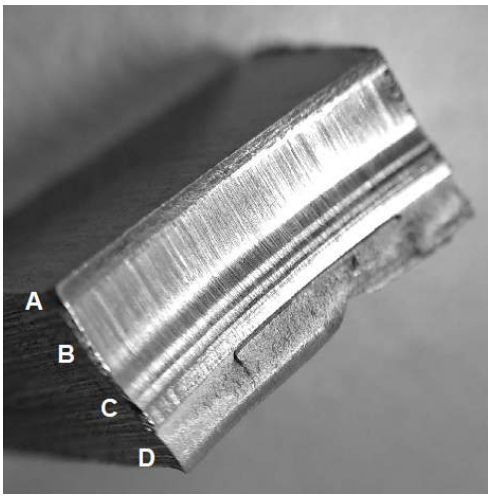

Figure 5.1: Photograph of the Case 12 sample that was used to study the different surface structures. Different zones are labeled accordingly.

The surface showed evidence of an initial adhesive behaviour that is responsible for the formation of scales situated in what will be designated as Zone A, which is where the squeezing punch makes the first contact with the sheet. In this zone, adhesion mechanisms happen because material that is pulled attaches itself to the squeezing punch at initial stages. As the downward movement of the tool continues, the adherent particles are squashed against the sheet inner hole surface, forming the so called scales, as seen in Figure 5.2.

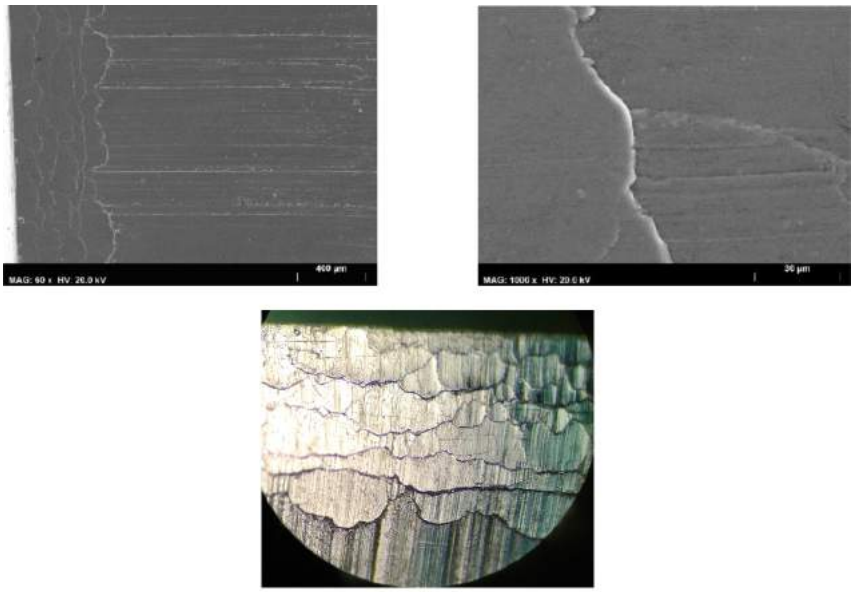

Figure 5.2: SEM fractography images on the top with magnifications of 60x and 1000x that show the scales and the inside of a single scale. Below, a microscopy (50x magnification) picture that shows the adhesion results that are formed.

Zone B starts when the shear mechanism begin to make its effect, this is, when the accumulated ductile damage reaches a critical value that initiates shear mechanisms. Note that once critical damage is surpassed, material on the sheet surface separates from material in the shear band located under the cross-section recess corner of the punch and forms a new fresh surface that allows the tool to continue its downward movement. This shear mechanism tends to create typical dimples that are ovally shaped, however, observing the SEM images, the results didn't show that phenomena. The explanation for this lies on the fact that, as the squeezing punch descends, material adheres to the punch by cold welding and is dragged along the new surface, eliminating the shear dimples that were created. Because of this and as can be seen in Figure 5.3, the surface shown is very smooth because of the severe wear damage.

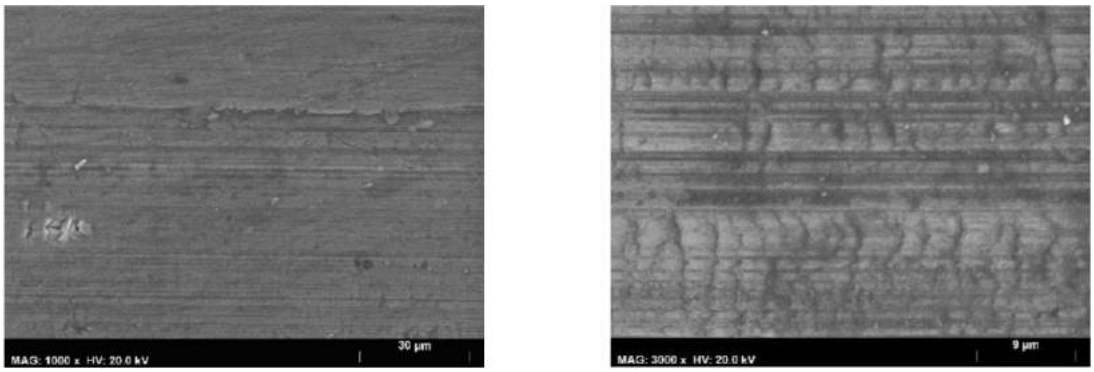

Figure 5.3: SEM fractography images of Zone B. A region near the transition to Zone C is shown to the left , showing thus a more rugged surface, as opposed to the picture on the right, that shows a smooth surface.

Zone C marks the transition between the penetration and the end of the process and, as can be seen, the surface is similar to what is observed in Zone B apart from a large bump that is encountered. That phenomena happens because, for large squeezing depths, there is an increase of the outward flow of material that originates a large clearance between tool and sheet which is seen in the image as a large bump. To show this, SEM images and numerical results for various depths are shown below in Figure 5.4 where the large clearance is exposed explaining thus the bump feature.

Zone D isn't characteristic to the process itself as it resulted from the separation of the squeezed sheet material in order to be able to put the sample through microscopic assessments. However, this region of the surface presents itself as useful as it shows the typical dimples formed by tension separation. In Zone B, similar dimples with a slightly more oval shape were expected to be seen, typical of shear mechanisms, instead of the circular that are shown.

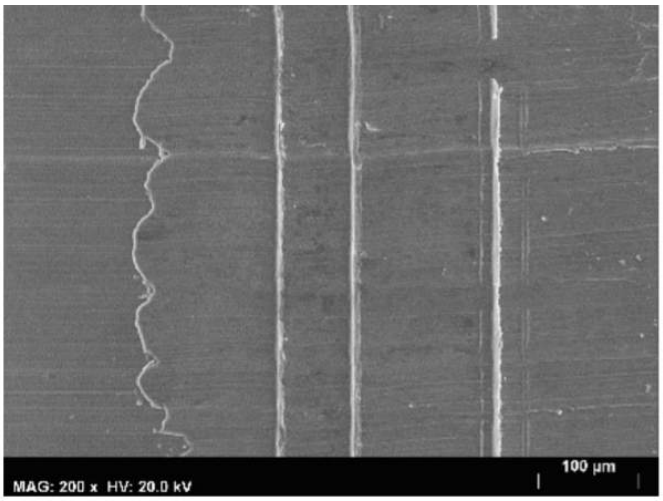

(a) SEM picture of the transition Zone C

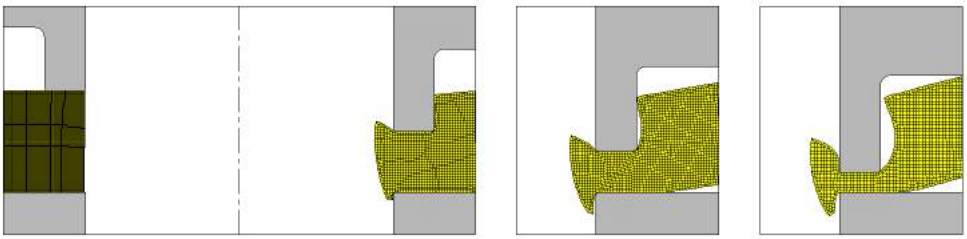

(b) Finite Element meshes for different squeezing depths showing the clearance between tool and sheet. This clearance is responsible for the noticeable bump in SEM imaging.

Figure 5.4: Experimental and Numerical Results

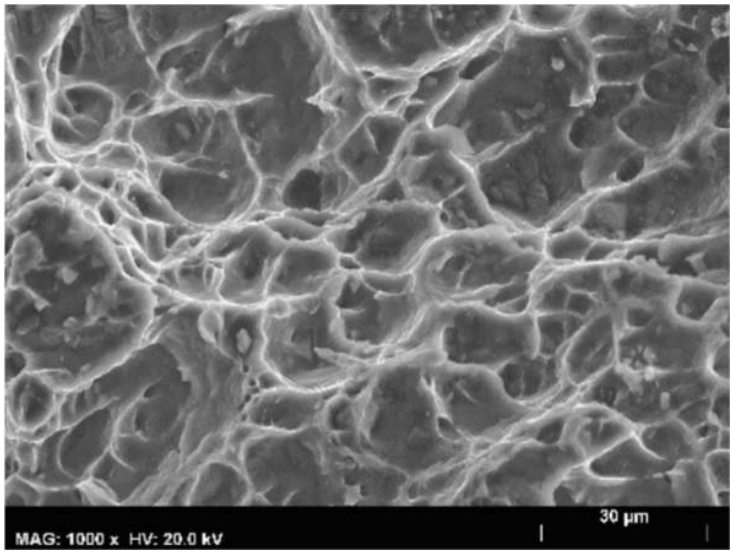

Figure 5.5: SEM picture of Zone D.

5.1.2 Experimental and Numerical Results

Numerically, it was also possible to prove that shear stresses control the mechanism of formation of new surfaces and, in order to evaluate its magnitude and importance on the process, a comparison of results between the upset compression of rings and the annular sheet squeezing was made.

In order to single-out the contribution of shear mechanisms to the process, the tests performed included cases with and without an outward constraint. These tests were later compared to the case with an adjacent material constraint that guaranteed the existence of shear stresses (annular sheet squeezing). Below, the 3 tests performed and their numerical results for distortion γ and shear stress τ, are displayed.

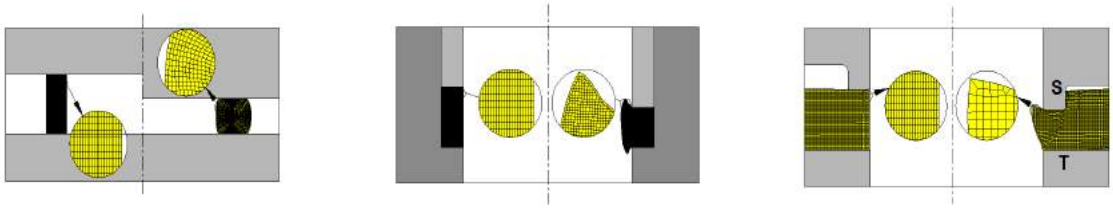

(a) Initial and Final mesh for Case 2R, Case 2RC and Case 4S, respectively.

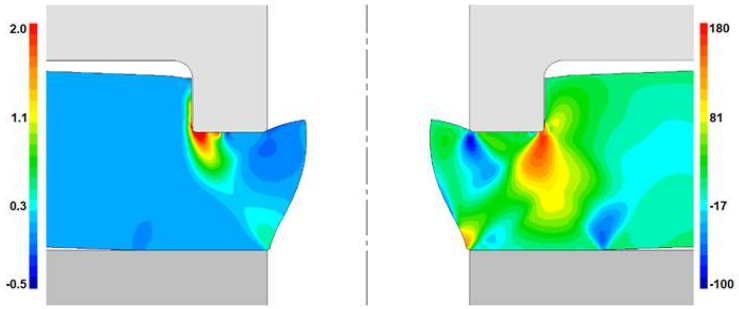

(b) Finite element predicted distribution of distortion on the left and shear stress (MPa) on the right.

Figure 5.6: Experimental and Numerical Results

The images shown in Figure 5.6 show that indeed the new surface is formed by shear stresses. However, results for the force-displacement evolution of the 3 types of tests performed show an interesting result. It's important to note that the evolution of Case 2R (no constraint) is almost the same as the evolution of Case 4S, while Case 2RC shows higher values of force, as could be expected. In fact, what is shown by these evolutions is nothing more than the fact that shear stresses don't have a significant impact in the process' force-displacement evolution as it's known that Case 2R doesn't have any shear stresses and Case 4S has shear stresses due to the adjacent material constraint, and it's seen that both have the same force-displacement evolution.

This allowed to conclude that the shear stresses have no impact on the process, namely regarding the energy needed to secure the joint and can, thus, be neglected as the results in Figure 5.7 show that there is no difference between cases with adjacent material constraint and no constraint.

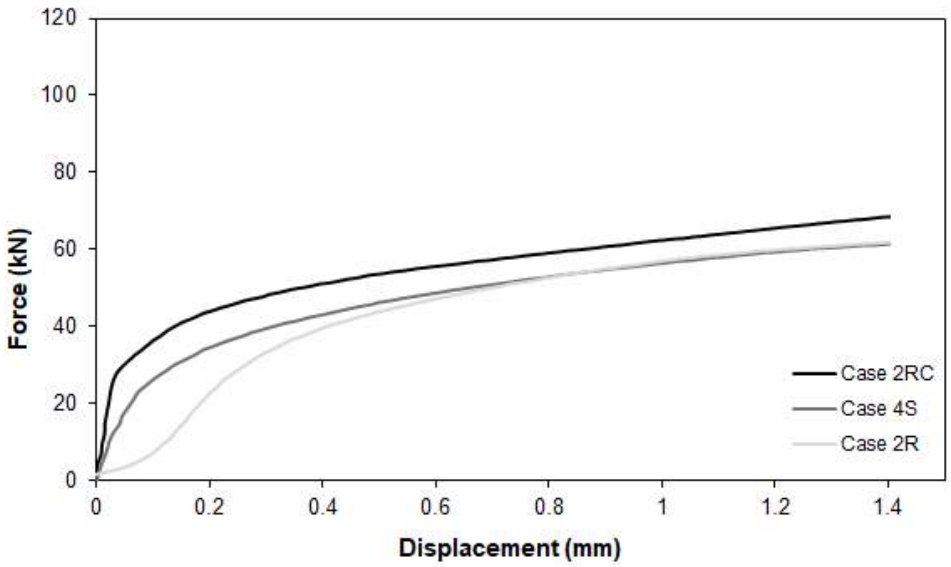

Figure 5.7: Experimental results for the force-displacement evolutions for Cases 2R, 4S and 2RC evidencing that the shear stresses aren't relevant to the process.

5.1.3 The Shear Stress Importance

The development of the new joining by forming process allowed concluding, as seen above, that shear stresses exist and are responsible for the formation of new surface, being of vital importance for the process as, without shear stresses, the squeezing punch could never advance and squeezing depths would be null. However, and as seen with both numerical and SEM fractography results shown above, the shear stresses can be neglected as they don't impact on force-displacement evolutions.

5.2 Influence of the Cross-Section Recess Length *l*

5.2.1 Experimental and Numerical Results

The results obtained experimentally and numerically allowed the identification of a strong correlation between the type of deformation observed in both the tube and the sheet and the cross-section recess length *l*. For different values of this parameter, various forms of inner tube beads were observed, indicating that in some cases deformation only occurred locally, while in other cases (for larger values of *l*) the deformation was homogeneous. The obtained sheet-tube connections are represented below, together with the cross section geometries photographs and FEM results. The observation of the different modes of deformation were obtained by numerically plotting the effective strain rate (s^{-1}).

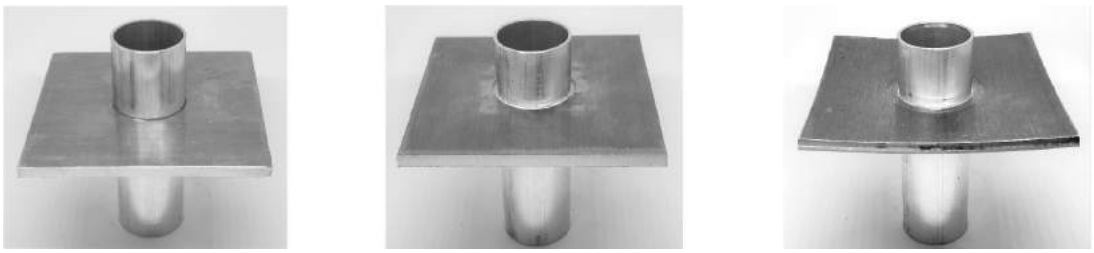

(a) Photographs of sheet-tube connections for cases 1, 4 and 7 of Table 3.3.

(b) Photographs and finite element predicted geometries of the cross sections of the sheet-tube connections shown in (a).

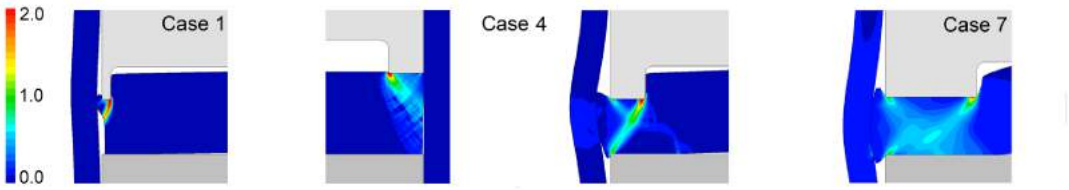

(c) Finite element predicted distribution of effective strain rate (s-1) for the sheet-tube connections shown in (a).

Figure 5.8: Experimental and Numerical Results

As can be seen in Figure 5.8, it is possible to distinguish three different types of deformation modes. In Case 1, the deformation is inhomogeneous and in Case 7 the deformation is completely homoge-

neous. Case 4 shows an intermediate situation where both flow types are encountered at some point of the process. Because of this, it became crucial to define a criteria that translated these three types of deformations and allowed the optimization of the cross-section recess length parameter.

5.2.2 Modes of Deformation and the Optimum Cross-Section Recess Length *l*

The different modes of deformation are directly related to the way material flows inside the sheet thickness, that again depends on the chosen value for the cross-section recess length. Those differences can be quantified by a deformation-zone parameter $\Delta = t_s / l$ that is defined as the ratio between the sheet thickness and the cross-section recess length.

In the work of Caddell and Atkins [30], it was observed through microhardness tests that the outer layers of drawn wire were more severely work hardened than the inner layers, showing inhomogenous flow. This led to the creation of a geometric parameter that quantified the relation between inhomogeneous flow and redundant work. Later, Hill [31] showed that different slip-line fields could be created resulting from the variation of the geometrical conditions in compression operations and it's possible to confirm those slip-line fields in Figure 5.8. It's because of these two works that, Alves et al. [28] defined a deformation-zone parameter Δ to allow a relation between inhomogeneous plastic flow and redundant work. This possibilitated the differentiation of either homogeneous and inhomogeneous flow in the sheet thickness and more importantly, helped to quantify these differences in order to simplify the development of the joining by forming process and also achieve the optimization of the cross-section recess length. Taking the experimental work plan shown in Table 3.3, the parameter Δ varies between 1 and 10.

The transposition of the deformation-zone parameter concept to the joining by forming process allowed to conclude that for large values of Δ, plastic deformation is localized and does not extend through the sheet's thickness (inhomogeneous flow shown by Case 4 in Figure 5.8). This mode of deformation, hereafter designated as Mode I, will promote a small amount of material to flow against the tube, thus creating small inner tube beads that compromise the joint's strength. Hence, it can be said that joints made by Mode I are not optimal.

Oppositely, for small values of Δ, plastic deformation occurs through the whole extent of the sheet's thickness since the start of the process (Case 7 of Figure 5.8), creating a mode of deformation that will hereafter be designated as Mode III . In this case, the deformation is homogeneous and a large amount of material will flow towards the tube but with a slight problem that is created which compromises the quality of the joint. This problem is associated with the decrease of outward constriction by adjacent material which will allow for more outwardly flow that will, consequently, result in a very noticeable and excessive sheet bending that compromises the joint's quality. It becomes also safe to say that joints produced by Mode III deformations aren't optimal either.

The explanations provided for Modes I and III allowed concluding that the optimal situation for this process would be a mode of deformation that promoted both inhomogeneous and homogeneous flow, as opposed to only one of them. This led to the mode of deformation hereafter designated as Mode II that actually proved to include the dual deformation type (inhomogeneous and homogeneous). This is shown in the initial step and final step of Case 4 in Figure 5.8. It was possible to, in this case, obtain a sound joint because an optimal amount of material was able flow against the tube, thus creating well dimensioned inner tube beads while, at the same time, maintaining a fair amount of adjacent material that provided reasonable outwardly constraint and prevented excessive sheet bending (caused by outwardly material flow, as seen for Mode III).

Another interesting discovery was made and confirmed that the existence of both inhomogeneous and homogeneous deformation was of paramount importance in order to produce acceptable joints. The results are shown in the plot of the inner radius percentage reduction, given by $(r_0 - r_b) / r_0$, for different values of the deformation-zone parameter Δ. It is shown that maximum tube bead dimensions are obtained for values of Δ equal to 2.5, that corresponds to a cross-section recess length of approximately 2 mm, and most importantly to a case of Mode II. What's interesting is that even though it would be initially expected that larger inner tube beads would be created for cases in Mode III, as more material flows against the tube, a different outcome is obtained. The results show that joints obtained with Mode II are the ones presenting the biggest inner tube beads.

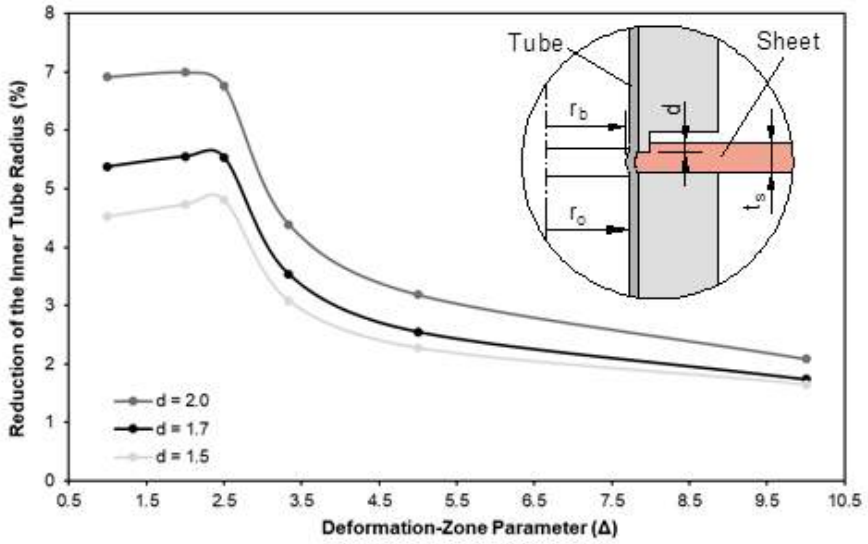

Figure 5.9: Finite element predicted reduction of the inner tube radius as a function of the deformation-zone parameter for different maximum depths of squeezing . The enclosed scheme shows a detail of the tube joint with appropriate notation.

5.3 Influence of the Squeezing Depth *d*

5.3.1 Experimental and Numerical Results

The experimental and numerical simulations made for various values of the squeezing depth *d* showed the enormous influence this parameter has on the inner tube bead dimension. Below are the pictures of the experimental and FEM tests for Cases 8, 9, 10 and 12.

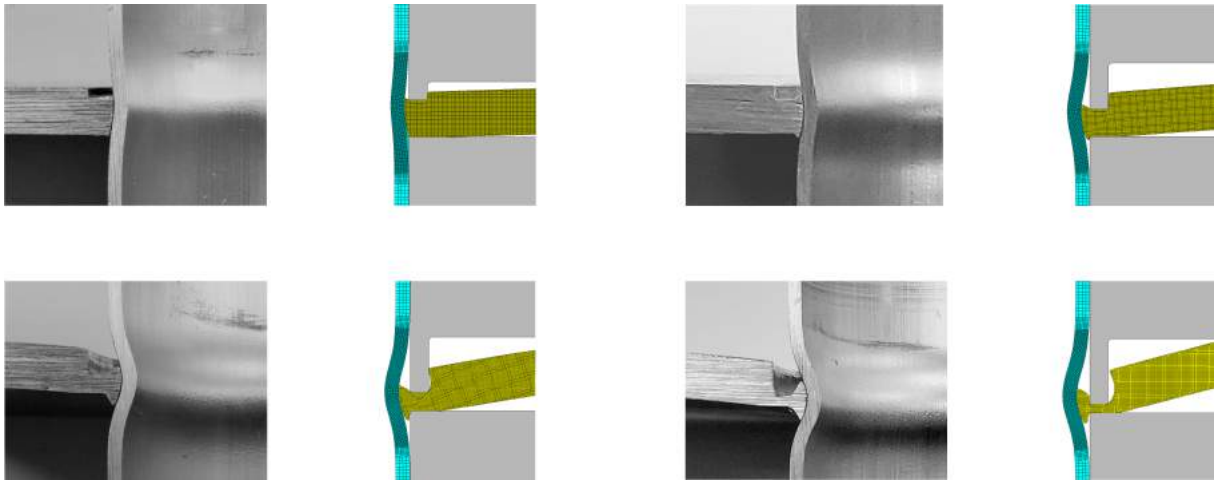

Figure 5.10: Experimental and finite element predicted cross sections of sheet-tube connections produced for Cases 8, 9, 10 and 11.

5.3.2 Inner Tube Bead and Destructive Load Interdependence

It is verified that there is an increase of the inner tube beads when higher squeezing depths are used and this increase has a positive influence on the joint's quality as it can withstand a higher loads before its failure because of the larger inner tube beads. However, it was also observed that there exists a critical value for the squeezing depth from which the joint no longer can withstand higher loads and actually fails for much lower values of force. The reason for this lies on the fact that, for squeezing depths that go beyond the critical value, the not squeezed material that forms a resisting section becomes too small and failure occurs much more easily. It becomes evident that a compromise solution must be found between the thickness of the sheet and the chosen value for the squeezing depth. In fact, the optimal value for the squeezing depth was shown to be of approximately 3.7 mm, for the tested setup.

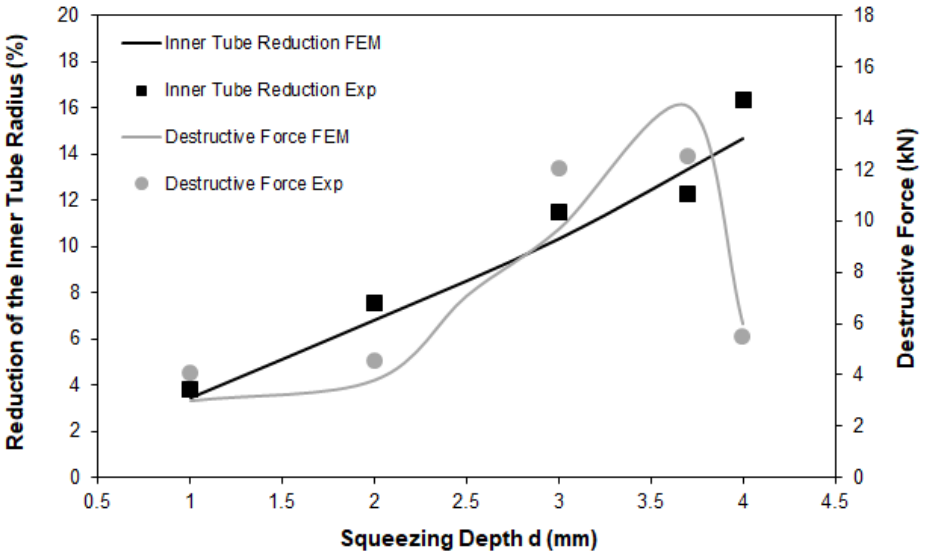

Figure 5.11: Influence of the squeezing depth *d* on the quality and strength of the sheet-tube connections.

5.4 Interdependence Between *l* and *d*

5.4.1 The Neutral Region Position Shift

The neutral region is defined as the separation between material flow that goes towards the tube and away from it. It becomes safe to say that at some region the flow velocity is null, creating the already referred neutral region. Throughout the tests performed by Alves et al. [32] plots of the horizontal flow velocity were used in order to verify a shift of position of this neutral region. This shift would later prove to have an enormous impact on the optimal value of the cross-section recess length that could be used. In other words, for different squeezing depths, the optimal cross-section recess length values differ, caused by the neutral region shift.

As can be seen below, a variation of the neutral region's position occurs for any change made to either one of the two parameters (*l* or *d*) and will cause different material flows that will have a direct influence on the amount of material that flows towards the tube and creates the inner tube bead. The results show that in fact, both the cross-section recess length and the squeezing depth are interdependent, and a compromise solution between both exists.

Numerically, it was seen through the finite element predicted distribution of the radial flow velocity that for various cross-section recess lengths and squeezing depths, different behaviours could be identified. Recovering the already discussed parameter Δ, it was possible to conclude that for large values of Δ, the neutral region had a concave shape and didn't shift its position relative to the squeezing punch's

corner regardless of the squeezing depth value whereas for small values of Δ, the neutral region took a linear shape and proved to be very sensitive to position shifts.

(a) Radial flow velocities for cross-section recess length equal to 0.5 mm and squeezing depths equal to 0, 0.5, 1 and 2 mm.

(b) Radial flow velocities for cross-section recess length equal to 1.5 mm and squeezing depths equal to 0, 2, 3 and 4 mm.

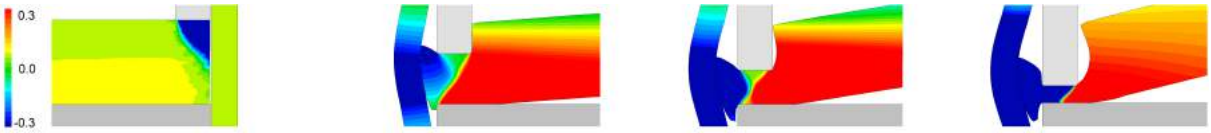

(c) Radial flow velocities for cross-section recess length equal to 2 mm and squeezing depths equal to 0, 2, 3 and 4 mm.

(d) Radial flow velocities for cross-section recess length equal to 5 mm and squeezing depths equal to 0, 0.5, 1 and 2 mm.

Figure 5.12: Radial flow velocities for different squeezing depths for each cross-section recess length.

Observing the figures, 3 types of neutral regions could be observed and it's important to note that inward flow is painted with cold colours and outward flow is painted with warm colours. For large values of Δ (Figure 5.12 (a)), where the mode of deformation is described as Mode I and thus, entirely inhomogeneous, the separation between inwardly and outwardly flow is assured through a stationary concave neutral region and once again, a very small amount of material is seen to flow against the tube creating non optimal joints.

For small values of Δ (Figure 5.12 (d)), the mode of deformation is described as Mode III and the flow is entirely homogeneous (Figure 5.12 (d)). In this case, the neutral region has a linear shape and suffers a large displacement when the squeezing depth increases therefore negatively affecting the quantity of material flowing towards the tube as a significant amount of material flows outwardly, thus providing

smaller inner tube beads and, again, worse connections.

Interesting insights were provided by the figures representing cases for values of Δ that ensure Mode II deformation (Figure 5.12 (b) and (c)) and incorporates, as known, both inhomogeneous and homogeneous flow. Mainly, these insights related to the different material flow behaviour and the impact it had in the inner tube bead dimension. Looking at Figure 5.12 (b), it became evident that the neutral region remained in the same position until a large depth is attained, in this case, 4 mm. From this moment, a radical shift of the neutral region position occurred and the flow was completely altered. Interestingly, looking at Figure 5.12 (c), the neutral region position shift occurred differently than the one seen before. When the squeezing depth was equal to 3 mm, a noticeable dislocation of the neutral region happened, however, after a further increase of the squeezing depth, the neutral region returned to its original position assuring the inward flow of a large quantity of material. Interestingly, it was seen that even though this position shift occurred in very little time, it had a large impact on the joint's quality because the sudden dislocation happened in a stage of the process where still a lot of material could flow towards the tube and therefore significantly reduced the quantity of inward flow. In the end, it was possible to see that smaller inner tube beads were formed than the ones created in the case depicted in Figure 5.12 (b), explained by the fact that in such case the shift occurred in later stages of the process and didn't interfere with the quantity of material that was directed towards the tube. This allowed to say that because of the neutral region position shift, caused by the squeezing depth, a new optimal cross-section recess length was found. Again, Hill [31] helps explaining that for different values of *l*, different slip-line fields are created and therefore, different behaviours are encountered in the neutral region, directly affecting the flows of material and consequently the inner tube bead radius.

5.4.2 Optimal *l* for different values of *d*

The studies mentioned above helped Alves et al. [32] to reach the conclusion that indeed, depending on the combination of these two parameters (*l* and *d*), different optimal solutions for this new process would surge. This is made quite clear in Figure 5.13, in a graph that shows the relationship between the reduction of the inner tube radius, the cross-section recess length and the squeezing depth. It can be seen that when the squeezing depth increased its value, the optimal cross-section recess length value diminished, proving that the hypothesis put above is valid.

Moreover, Figure 5.13 shows that when squeezing depths are maintained under 2 mm, the maximum inner tube radius reduction occur for *l*= 2 mm. On the contrary, when squeezing depths are increased to 3 mm and 4 mm, the maximum reduction of the inner tube radius occurs for *l*= 1.5 mm, proving once again what is stated above is correct. There is a clear tendency for a smaller optimal cross-section recess length when larger squeezing depths are chosen.

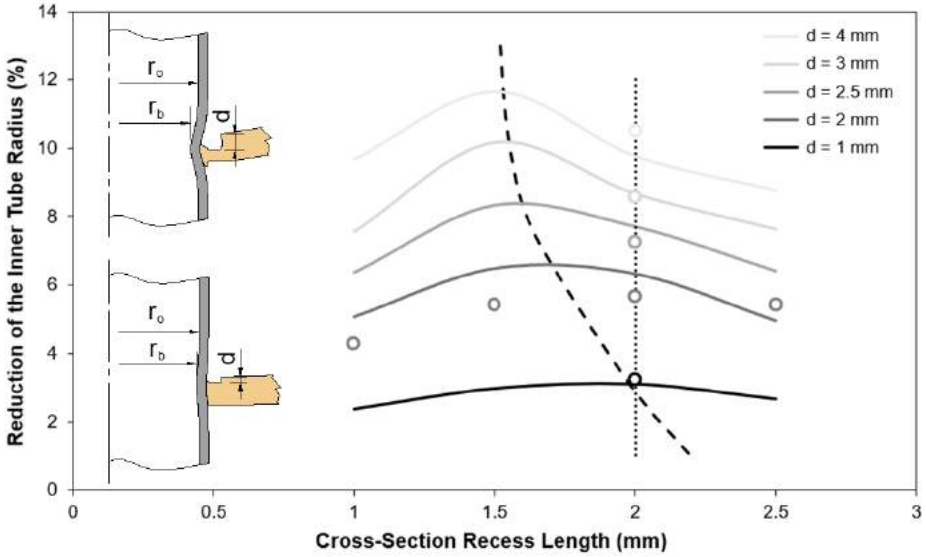

Figure 5.13: Reduction of the inner tube radius as a function of the cross-section recess length of the punch for different values of the squeezing depth. Note that experimental values are shown with circles and cover two cases, one with a variable cross-section recess length and squeezing depth equal to 2 mm and the opposite.

5.5 Influence of the Tool's Inner Radius and Angular Inclines

In this section, three different parameters and their influence on the process were studied and it's important to note that only the surface contact incline α was performed experimentally while the lateral surface incline ϕ and the tool inner radius (offset) were performed numerically.

5.5.1 Tool Inner Radius by means of an Offset

As explained before, the idea behind the increase of the inner radius of the tool was to, by that, force the displacement of a rigid region of material of the sheet as opposed to only forcing flow of sheet material adjacent to the tube. Note that all the tests were performed for a constant cross-section recess length equal to 2 mm and the squeezing depth was varied. The resulting deformation is shown below in Figure 5.14.

Simulations showed that the tube inner beads created by this type of setup aren't significantly bigger than the ones created with an offset equal to 0 mm. The only case where the offset actually promoted some gain was for a value equal to 0.2 mm which, in reality, does not have as a significant relevance as it does not make any sense to talk about these kind of dimensions when associated with industrial practices and so, it's possible to conclude that from an industrial point of view, there would not be any advantage of using this parameter as opposed to what was the initial idea of a null offset.

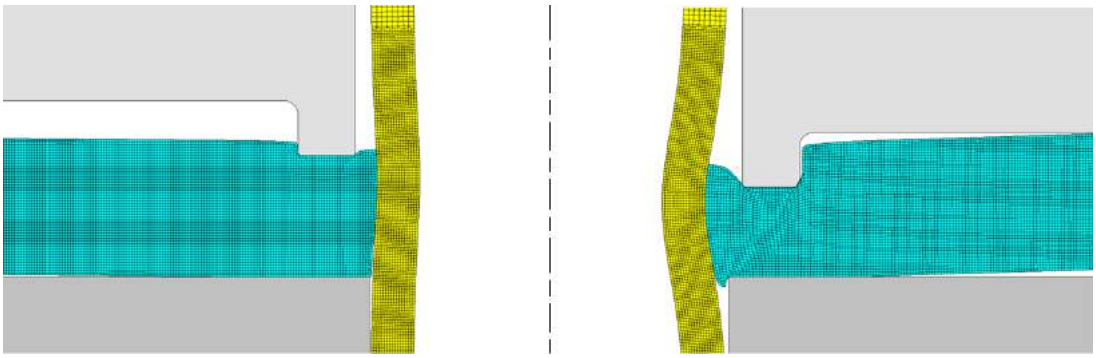

Figure 5.14: Finite element meshes for two distinct squeezing depths for a test with an 0.5 mm Offset

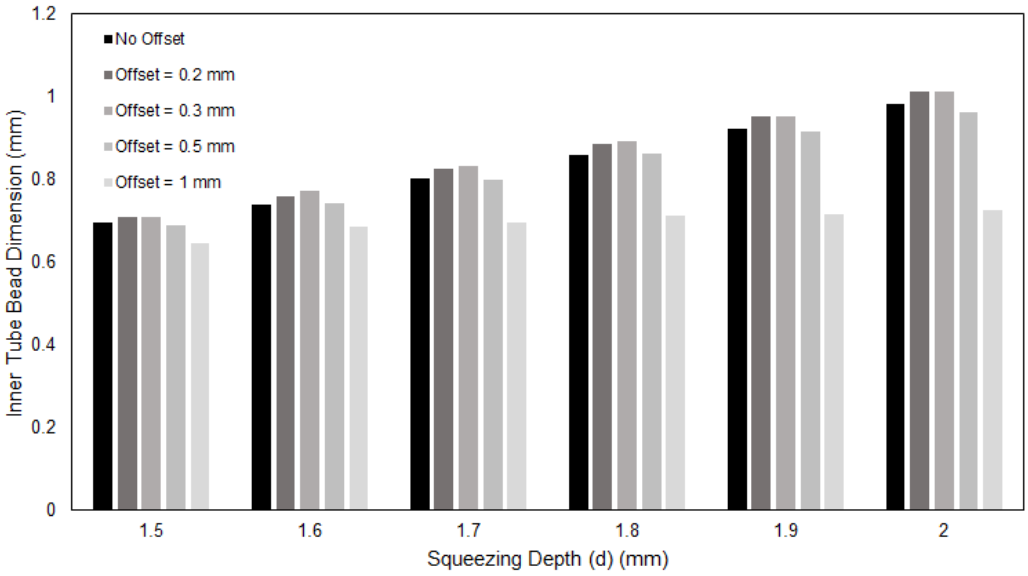

Figure 5.15: Inner Bead Dimensions for various Offset and squeezing depth values.

5.5.2 Contact Surface Incline - α and Lateral Surface Incline - ϕ

The addition of the contact surface incline aimed to help the flow of material towards the tube. However, the force-displacement evolutions for both numerical and experimental tests allowed to conclude that the necessary load to create the joints is lower than the Case 4, where α is equal do 0º concluding that, in fact, a smaller amount of material was being deformed and therefore not enough was flowing against the tube. In the end, this resulted in smaller inner tube beads and worse joints.

The addition of the lateral surface incline aimed to promote the flow of a solid portion of undeformed sheet material and, with that, achieve larger inner tube beads, however, results also show that there isn't any advantage in using this parameter as inner tube beads end up being smaller.

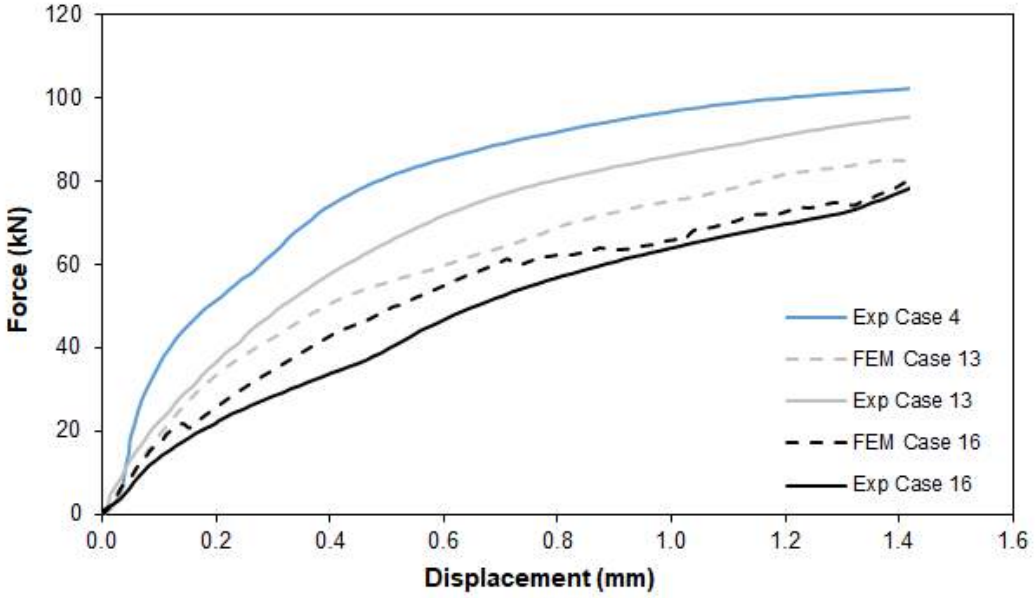

Figure 5.16: Experimental and finite element predicted value for the force-displacement evolutions with an angular incline on the contact surface of the squeezing punch.

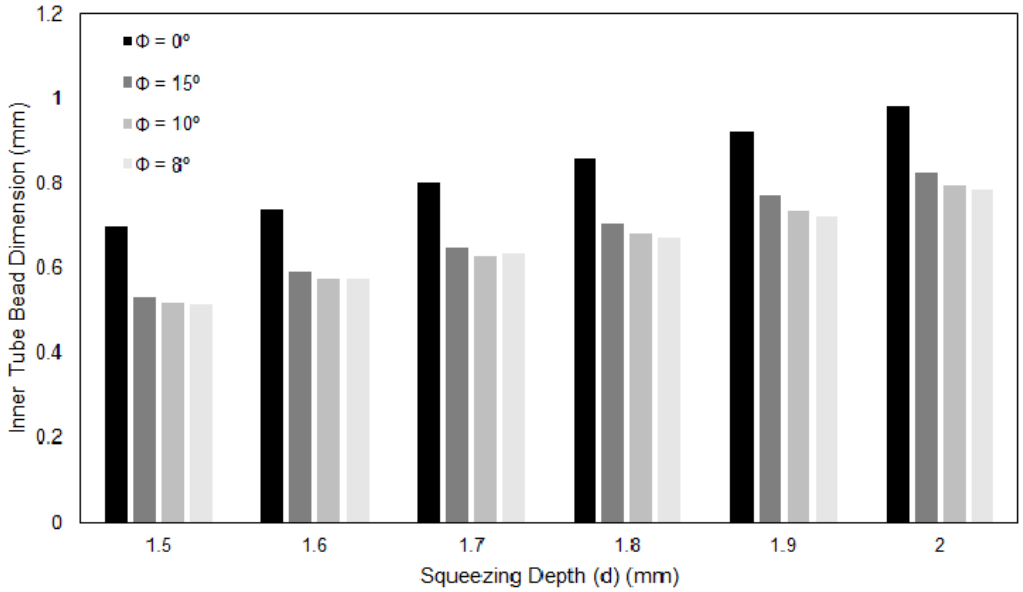

Figure 5.17: Inner Bead Dimensions for various lateral surface Incline and squeezing depth values.

5.6 Sheet Bending Behaviour

A characteristic process behaviour was observed in both experimental and numerical developments of this new process, designated as sheet bending. It was later proved that this behaviour depended on both the cross-section recess length and the squeezing depth, therefore, a suitable compromise solution between both parameters had to be assured, otherwise an accentuated sheet bending behaviour would occur. The bending of the sheet throughout the process happened due to the existence of a significant amount of outward flow and, as was seen above, for large values of the deformation-zone parameter (Δ, this behaviour would not happen because there wasn't a large amount of outwardly flow. However, joint's produced for these values of (Δ) had lower quality and mechanical strength. Nevertheless, for small values of the deformation-zone parameter, the amount of outward flow was seen to be large enough to cause excessive sheet bending. The existence of these two extreme cases eventually led to an optimal value for the cross-section recess length equal to 2 mm, that represented the ideal compromise solution between the joint's quality and the sheet bending behaviour.

Knowing the main reason behind the bending behaviour (outward material flow) and the fact that the sheet itself is responsible for providing the constraint that impedes the material from flowing outwardly, it became evident that for a certain sheet length (previously defined as s_L), the outward flow wouldn't reach the extremity of the sheet, resulting in a mitigation of the sheet bending behaviour. In addition to the ceasing of this phenomena, it was expected that the bending behaviour would become a local feature of the process, resulting in a wave alike deformation in the region near the tube while the rest of the sheet remained undeformed. In other words, for large values of s_L, it was be expected to see the sheet with the inner hole and the extremities at the same height and, near the squeezed region, a local bending in the form of a wave. However, with numerical tests performed to various sheet lengths, it was proved that, in fact, the sheet bending behaviour disappears for large lengths but never becomes a local feature, as the inner hole and the sheet extremities aren't at the same height.

Represented below, are the simulation results for three different sheet lengths (s_L). Note that, all simulations were performed with an equal squeezing depth. For the first two cases, it was possible to conclude that for values of s_L equal to 200 mm and 300 mm, there was still an excessive bending behaviour and therefore, the problem could only be solved for larger values of the sheet length. In the third case, where the sheet had a value of s_L equal to 600 mm, the bending stopped happening. The result showed that the sheet was flat in its extremity while bent near the squeezed region. However, the sheet's inner hole and extremities weren't at the same height, which comes to show that the bending behaviour is not a local feature, contradicting what was initially expected.

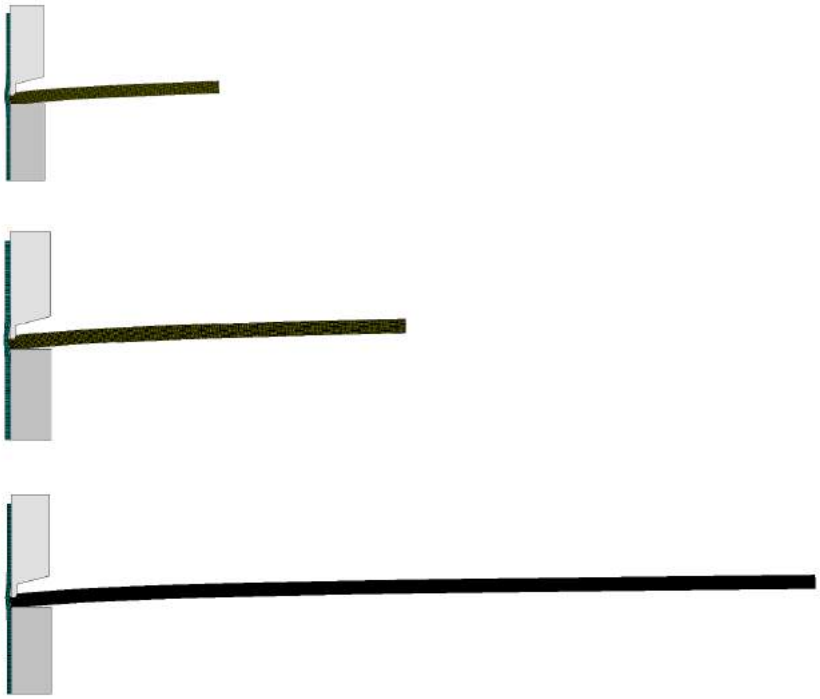

Figure 5.18: Finite Element predicted meshes for the final step of the operation. Tests performed to sheets with lengths equal to 200, 300 and 600 mm show a noticeable ceasing of the bending behaviour occurs for a sheet 600 mm long.

5.7 Inner Tube's Bead Stationary Behaviour

In the Process' Forces and Pressures Chapter (5.8), the force-displacement evolutions for large squeezing depths opened the possibility of the existence of a stationary behaviour in the process because it was seen that, at a given time, the force-displacement evolution was constant. Those observations led to a study that aimed the better comprehension of that stationary behaviour. That study was done through a simulation using a sheet with a thickness of 15 mm and the squeezing depth was set to 13 mm. The retrieved results are shown in Figure 5.19 and represent both the numerically predicted coordinates of the maximum inner tube bead point and the relation between the squeezing depth and the inner tube bead reduction. As can be seen, the fitting curves (represented as a dashed black line) in both graphs predict a clear tendency to the stationary behaviour of this process. However, it must also be noted that the stationarity could only occur for very large values of the squeezing depth. Looking from an industrial point of view, sheets with thicknesses in such large orders of magnitudes don't apply to the areas where this dissertation places its application span. It's possible to conclude that the stationarity does appear to exist but only for sheet thicknesses that are too large to even consider in this work.

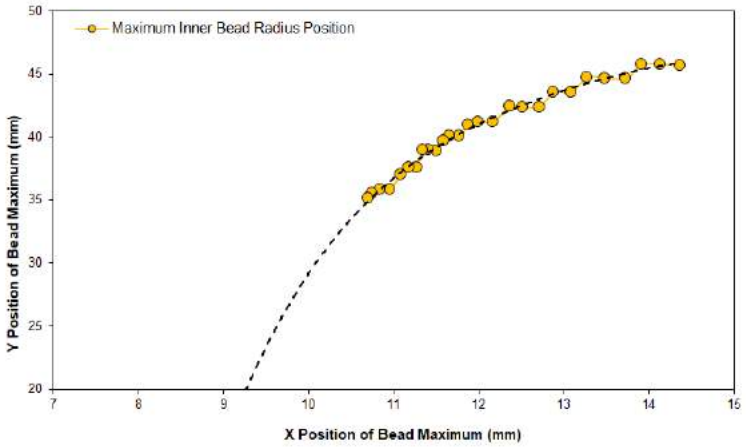

(a) Position of the inner tube bead's maximum point.

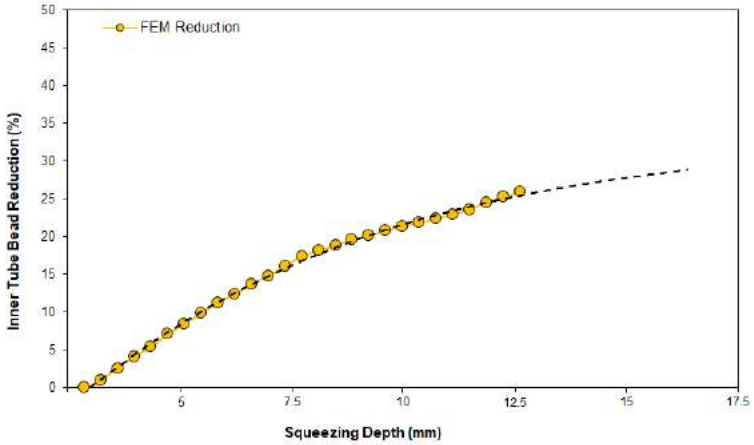

(b) Relation between the inner tube bead reduction and the squeezing depth.

Figure 5.19: Numerical Results for the Inner Bead´s stationary behaviour.

5.8 Process' Forces and Pressures

5.8.1 Experimental and Numerical Results

An important aspect when developing any new joining by forming process is understanding the evolution of the force throughout the process. This information will have clear implications on tool conception, equipment requirements, among others. The experimental and numerical results regarding the process' forces are presented below and show a good agreement, indicating an accurate choice and calibration of the main simulation parameters discussed in Chapter 4. As would be expected, when the cross-section

recess length is increased, the forces involved are larger as there is an increase of the tool contact area that will, in turn, deform more material and increase the forming loads. Shown in Figure 5.20, are the evolutions for Cases 1, 4 and 7.

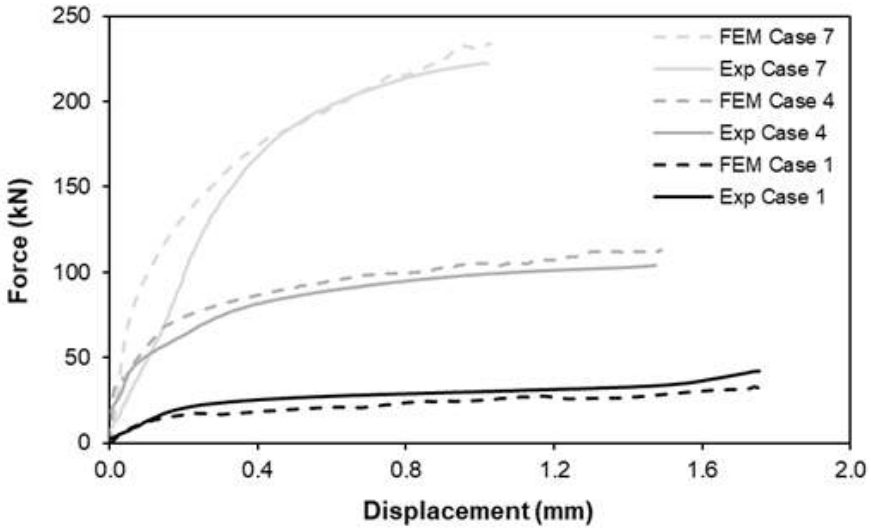

Figure 5.20: Experimental and finite element predicted value for the force-displacement evolutions.

The evolutions of force with displacement when the squeezing depth is increased for a constant cross-section recess length show three distinct zones, with unique behavioural characteristics. As shown in Figure 5.21 , the force starts by presenting an accentuated increase with displacement (region 'Z1'). Growth rates moderate for values of punch displacement approximately equal to 3 mm (region 'Z2'). Beyond this value (region 'Z3'), a faster growth rate is verified as the amount of sheet material left below the cross-section recess of the punch is very small and its flow becomes predominantly radial.

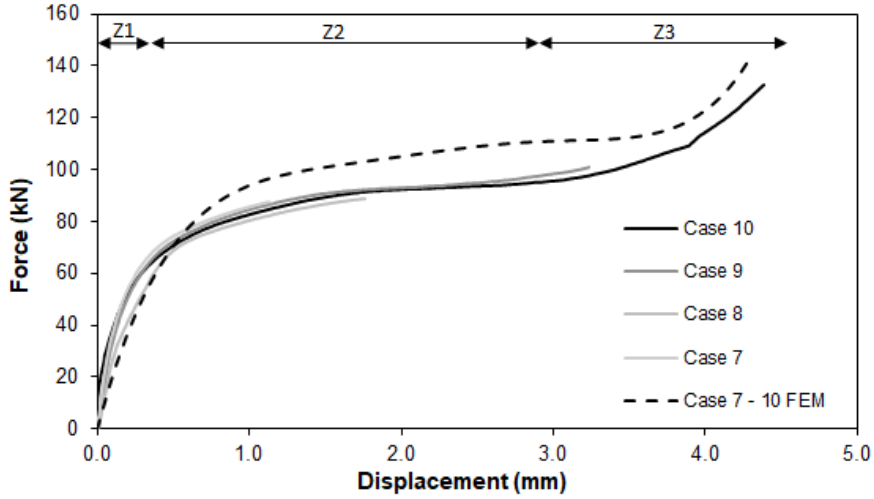

Figure 5.21: Experimental and finite element predicted value for the force-displacement evolutions.

5.8.2 Force Decomposition

In previous chapters, there was mention of the annular sheet squeezing experimental tests that were performed on standalone sheets. The aim of these tests was to discriminate the forces involved in the process and know the percentage of force that was required by the process to induce plastic deformation to the sheet and the tube.

After the experimental and numerical results were obtained, the initial hypothesis consisted of modeling the total force as a simple sum of the force necessary to squeeze the sheet (F_{sq}) and the force necessary to create the inner tube bead (F_{ib}). The force was thus defined as:

$$F = F_{sq} + F_{ib}$$

To sustain the validity of this simple model, experimental and numerical results are shown below in Figure 5.22 and Figure 5.23. These allow to conclude that, in fact, the force necessary to squeeze the sheet accounts for approximately 62% of the total force while the remaining 38% account for the amount of force necessary to form the inner tube bead.

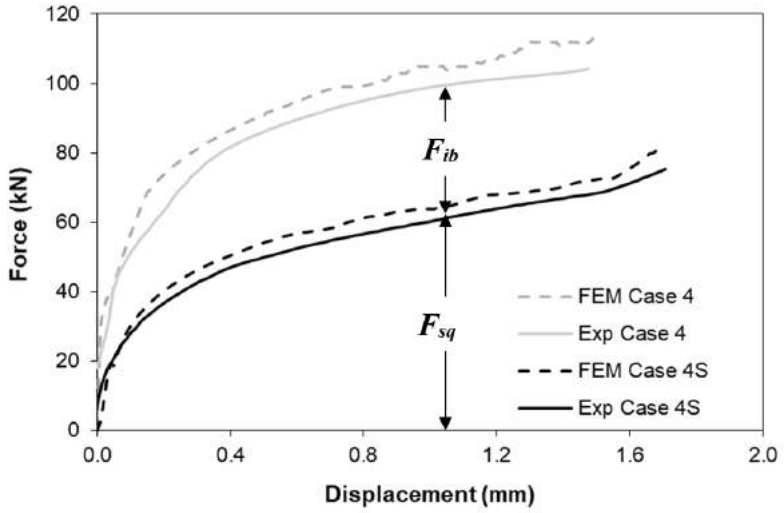

Figure 5.22: Experimental and finite element predicted value for the force-displacement evolutions.

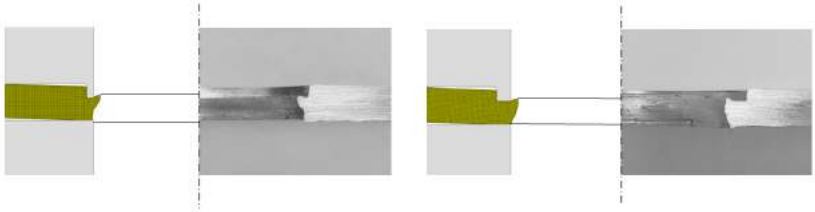

Figure 5.23: Photographs and finite element predicted geometries of the cross sections corresponding to the two test cases shown above.

A relation of F_{sq}/F_{ib} equal to approximately 1.6 is obtained and it is seen that the relation is roughly maintained for cases in Mode II of deformation as exemplified by Case 3 of Table 3.3 where, Δ is equal to 3.33 and the cross-section recess length is equal to 1.5 mm. As can be retrieved from Figure 5.24, the effective strain rate shows that also for this case, a Mode II deformation mode is obtained and the relation between F_{sq} and F_{ib} is maintained equal to approximately 1.6, proving what is stated above.

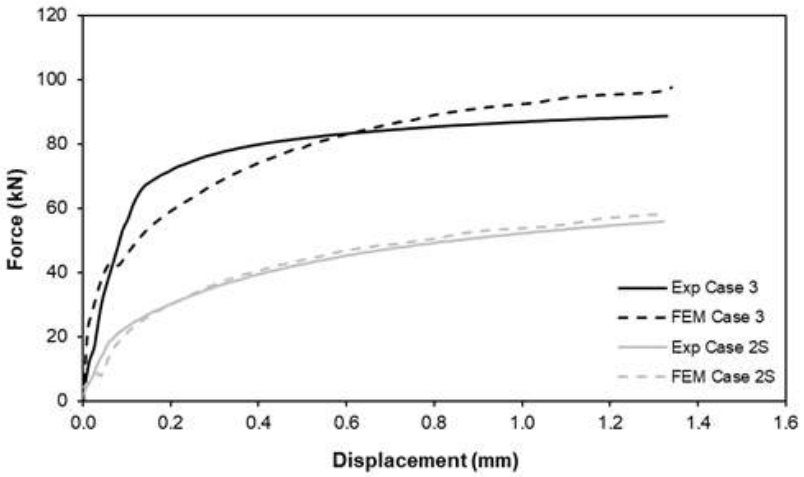

(a) Experimental and finite element predicted value for the force-displacement evolutions.

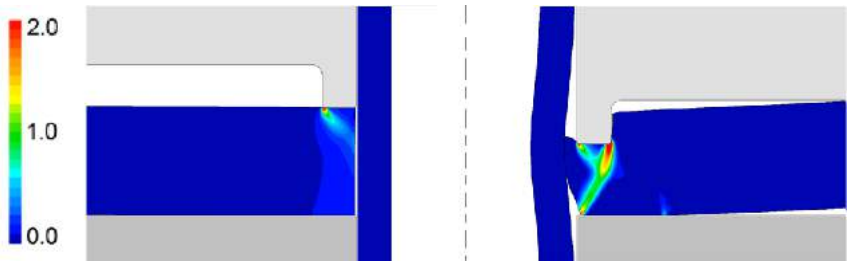

(b) Finite element predicted effective strain rate for Case 3.

Figure 5.24: Experimental and Numerical Results for the Process' Force Decomposition

However, this ratio is expected to vary as a function of the relative strength of the sheet and tube materials and in particular, should increase with the relative strength of the sheet material.

5.8.3 Maximum Tool Pressures

Determining the maximum pressure that acts on the tool is essential knowledge that allows accurate tool design. Returning to the deformation-zone parameter Δ, it is possible to establish some relations between the maximum tool pressure and that same parameter and, as seem, a good agreement between FEM and experimental data was obtained and the maximum pressure increases with up to a value of approximately 700 MPa due to redundant deformation, which becomes more important as plastic flow changes from homogeneous to inhomogeneous.

As shown in Figure 5.25, the increase of maximum pressure is qualitatively similar to that obtained in the slip-line compression of rectangular slabs by Hill [31], with an initial plateau followed by a region of monotonic growth. This allows concluding the initial model for the deformation-zone parameter is an adequate solution to quantify the already discussed influence of the cross-section recess length and the forces that are inherent to the process.

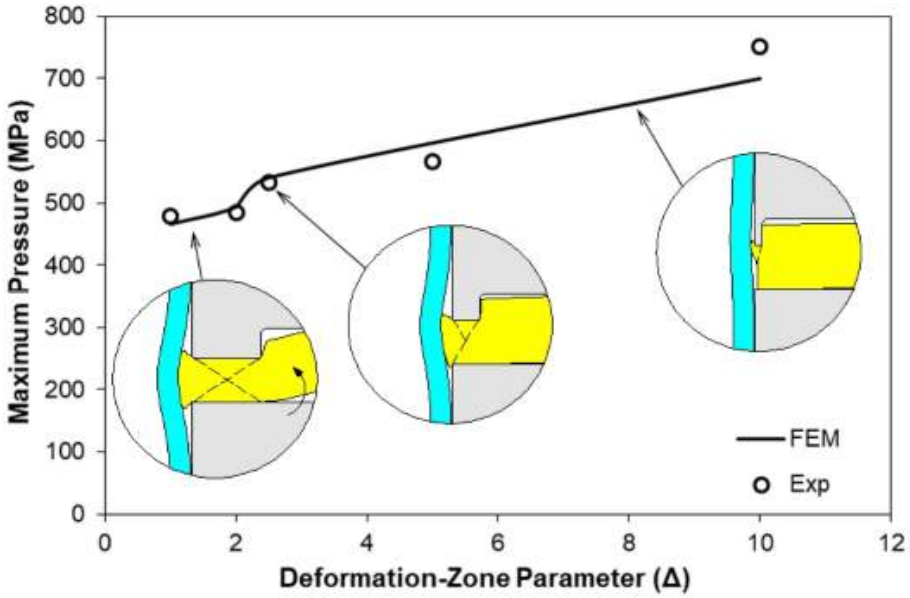

Figure 5.25: Experimental and finite element predicted value for the maximum tool pressure.

The results shown above also allow to conclude that, in fact, for very small cross-section recess lengths (translated in large values of the deformation-zone parameter), the maximum tool pressures are too large and could easily damage the squeezing punch. To effectively assure joints with those dimensions, the fabrication of the tool would imply different materials and heat treatments that, in turn, would add larger costs and complexities to the process.

5.9 Destructive Pull-Out Results and Joint Validation

The destructive pull-out tests were done in two opposite directions and it was initially expected that the joint's behaviour would differ according to the pull-out direction. The results ended up confirming that expectation as both experimental and numerical data showed a different maximum pull-out destructive load depending on the pull-out direction. The results are depicted in Figure 5.26.

The destructive pull-out tests showed an interesting feature of the process. The joint destruction force-displacement evolutions had great resemblance with that of an extrusion curve which allowed to conclude that the sheet actually functions as a floating die and the tube is forced to pass through it reducing its inner radius from r_0 to r_b. The load would increase until a peak was reached and from that point on, the load would decrease and reach a stationary behaviour, just like a normal extrusion curve would show.

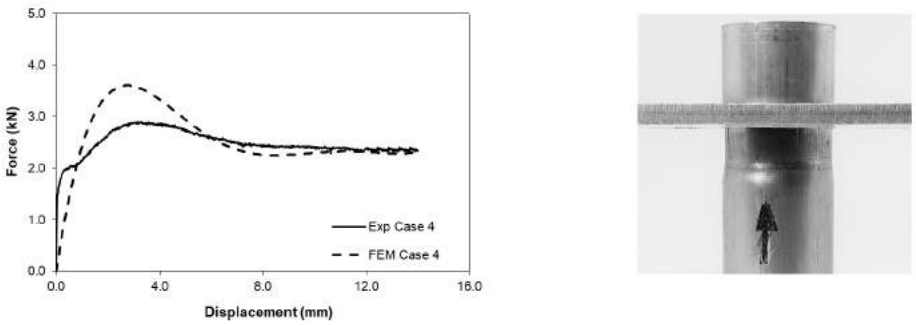

(a) Experimental and finite element predicted value for the force-displacement evolutions for the destruction test of Case 4 in the Bottom-Up direction and the respective experimental result photograph.

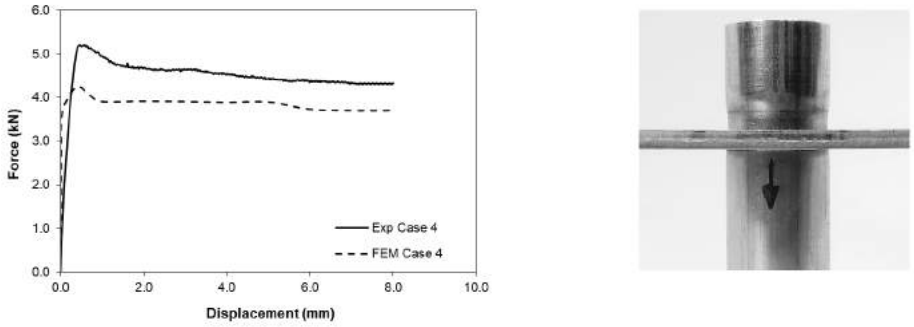

(b) Experimental and finite element predicted value for the force-displacement evolutions for the destruction test of Case 4 in the Up-Bottom direction and the respective experimental result photograph.

Figure 5.26: Experimental and finite element predicted value for the destructive pull-out load in different directions.

When the squeezing depth is varied, the destructive pull-out tests produce different results. Because the resisting sheet section is very reduced, the risk of rupture is increased and it becomes necessary to identify a threshold value for the squeezing depth that delimits the transition from a non-rupture to a rupture situation. Every destructive pull-out test shown below was performed the same way as the left image of Figure 3.9 depicts (Bottom-Up Direction).

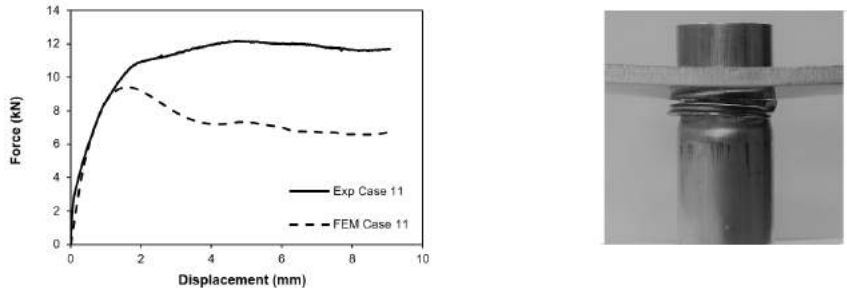

(a) Experimental and finite element predicted value for the force-displacement evolutions for the destruction test of Case 11 in the Bottom-Up direction and the respective experimental result photograph.

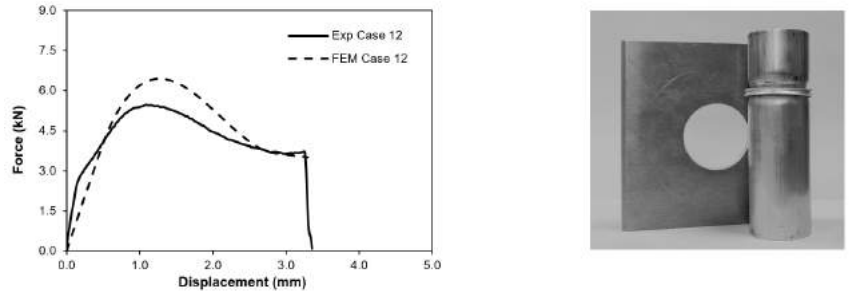

(b) Experimental and finite element predicted value for the force-displacement evolutions for the destruction test of Case 12 in the Bottom-Up direction and the respective experimental result photograph.

Figure 5.27: Experimental and finite element predicted value for the destructive pull-out load in different directions.

Observing the results for the destructive pull-out test for depths equal to 3.5 mm and 4 mm, it can be concluded that both cases suffered rupture. Nevertheless, it is immediately seen that for cases where the value of the squeezing depth is equal to 4 mm (Case 12), a total rupture of the joint occurs whereas, for depths equal to 3.5 mm (Case 11), the rupture isn't total. This observation allows the setting of a threshold value for the squeezing depth that separates cases where total rupture happens and where partial rupture happens. Depending on the application, the total rupture of the joint might be a non-negotiable requirement and for those cases, the used squeezing depths must be kept limited to values below 3.5 mm. Again, these threshold values only apply for the used setups.

6

Other Applications of Annular Sheet Squeezing

All the previous experimental test and numerical simulations were made using two different aluminium alloys. However, in order to validate this new concept and, more importantly, broaden its application window, sheets and tubes with other materials were used. Moreover it helped proving that this process is, in fact, a convenient replacement for conventional technologies that often fail to join dissimilar materials, namely welding.

The materials used were thoroughly characterized and their curves are presented below in Figure 6.1.

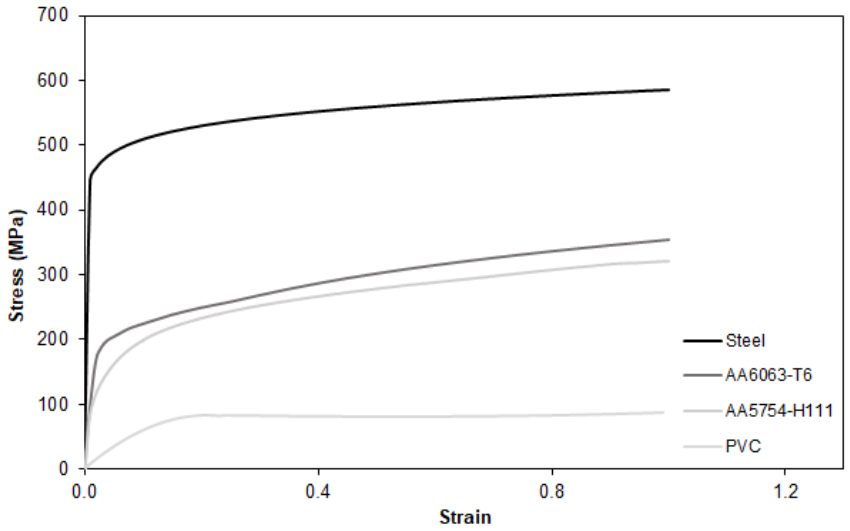

Figure 6.1: Flow Curves of the various materials used in the numerical work.

It was then possible to obtain multiple variations of the process. As shown in Figure 6.2, this new concept could be validated using various combinations of materials.

- Sheets - Aluminium; Tubes - PVC, Steel and Aluminium
- Sheets - PVC; Tubes - PVC and Aluminium
- Sheets - Litecore; Tubes - PVC

The key for this process to work is to assure that the strength of material that constitutes the tube isn't greater than that of the sheet because, in that case, the material of the sheet will flow outwardly instead of against the tube as it becomes energetically more favourable.

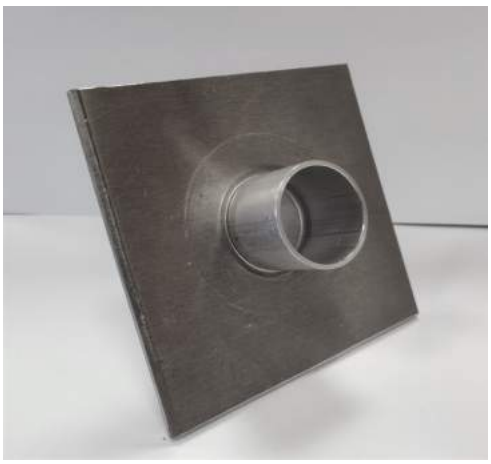

(a) Aluminium Tube and Aluminium Sheet.

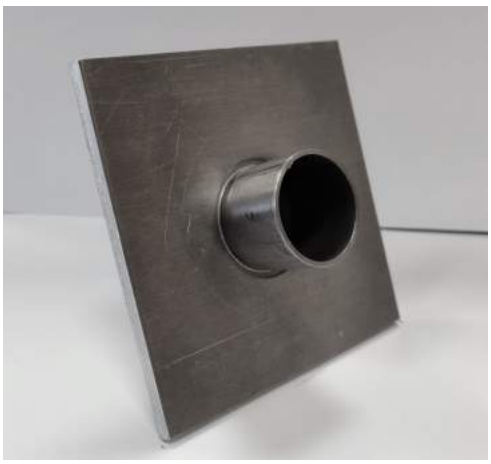

(b) Steel Tube and Aluminium Sheet.

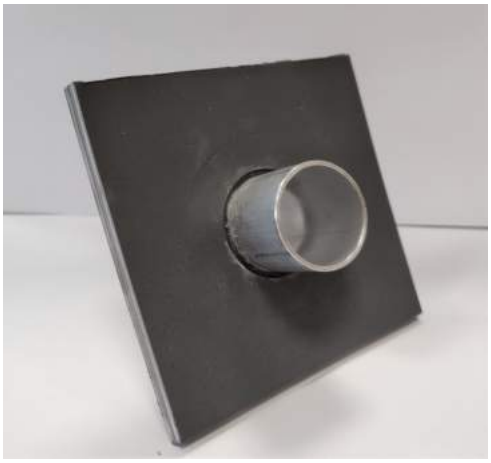

(c) Aluminium Tube and PVC Sheet.

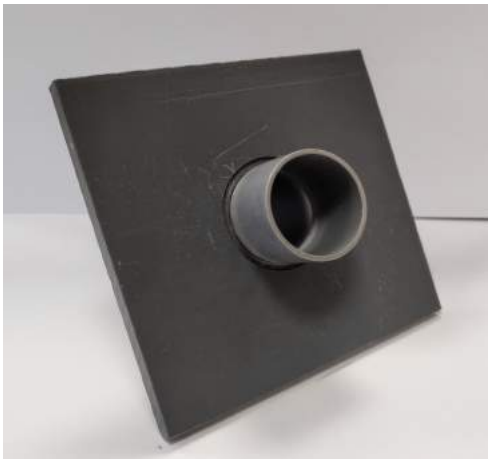

(d) PVC Tube and PVC Sheet.

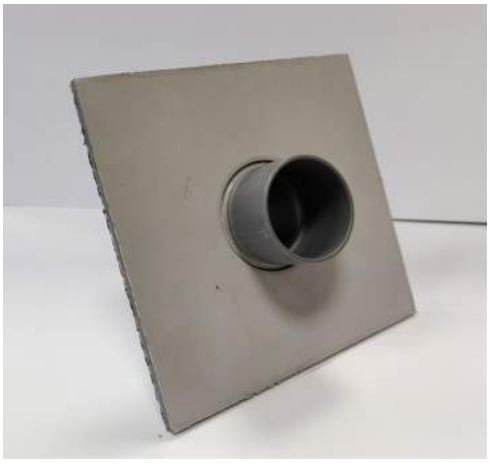

(e) PVC Tube and Litecore Sheet.

Figure 6.2: Applications of the process to other materials.

7

Conclusions and Future Work Perspectives

Contents

7.1 Conclusions

The development of this new joining by forming process results from a different perspective that was given to sheet-tube connections. Up till now, and as was described in Chapter 2, the joining by forming processes that surged focused on deforming the tube against the sheet. This led to many processes needing more than one operation in order for a joint to be assured. The only exception was the single stroke techniques proposed by BMW [10] and Alves et al. [17]. However, both single stroke techniques focused on Compression Beading which, as was seen, caused problems when applied to materials with low fracture toughness. This dissertation solves the problems obtained with Compression Beading and at the same time, secures joints with a single stroke operation. The concept focuses on performing the sheet-tube connections by deforming the sheet instead of deforming the tube. This work also shows that sheet-tube connections can be performed using less than 110 kN, a small load value, that shows the energy saving advantage of this new procedure. Moreover, the versatility of this new technique is shown by the numerous applications done with different materials other than aluminium alloys.

Fixing a sheet to a tube by annular sheet squeezing involves creation of a new surface by in-plane shear. The surface is formed ahead of the cross-section recess corner of the punch and its morphology mainly consists of grooves parallel to the punch moving direction. The grooves are caused by fragments that detached from the sheet during crack opening (surface formation) and subsequently adhere to the punch by cold welding. It was concluded that in the formation of a new surface, shear stresses existed but didn't have any impact in the process' total force and thus, aren't responsible for any energy loss in the process.

It was possible to conclude that the main parameters to be considered are the cross-section recess length l and the squeezing depth d. These two parameters proved to control the entire process and compromise solutions between both must be assured in order to obtain sound joints.

Regarding the cross-section recess length parameter, it was possible to conclude that the ideal value for this parameter was a compromise situation between fully inhomogeneous material flow (obtained with small values of l) that was resulted in an insufficient amount of material to flow against the tube and fully homogeneous material flow (obtained with large values of l), responsible for a excessive of outwardly flow that caused an accentuated sheet bending effect. This was defined through the Deformation-Zone Parameter Δ, that successfully characterized the plastic flow inside sheet thickness. The optimal value for found the cross-section recess length was to be 2 mm, corresponding to a 2.5 value for Δ, that corresponded to a Mode II deformation.

Looking at the squeezing depth parameter, it was found that larger inner tube beads were created for larger values of d. This would mean that, the larger the squeezing depth, the better the joint's performance in the destructive pull-out test. However, because there is a decrease of the resisting section for larger depths, being found that the optimal depth for the process was 3.7 mm. This squeezing

depth allowed for an increase in both the inner tube bead radius and the pull-out load. For larger depths, the pull-out load fell abruptly as the resisting section didn't have the appropriate dimensions, leading to the complete rupture of the joint.

Interestingly, the cross-section recess length and the squeezing depth were found to be interdependent. This was explained by plotting the horizontal material flow velocity. Because of the observed changes in the way material flows, depending on both the cross-section recess length and the squeezing depth, it was concluded that for larger squeezing depths, the optimal value of *l* would decrease to about 1.5 mm. This happened because, for larger squeezing depths, a shift of the neutral region's position caused a larger amount of outwardly flow, resulting in smaller inner tube beads. For a smaller cross-section recess length, the increase of the outward flow for larger depths was attenuated, becoming therefore a new optimal *l* (1.5 mm), smaller than the 2 mm cross-section recess length that was taken as the optimal value up till that point.

Every other study performed based its conclusion on these two main parameters. Knowing that outward flow is the cause for sheet bending and that the sheet itself provides the constraint that stops the material from flowing outwardly, a conclusion was obtained regarding the sheet length that stopped the bending behaviour from happening. In fact, this behaviour stops for a 600 mm long sheet. From this point on, the bending only occurs near the squeezed region of the sheet.

When the destructive pull-out tests were performed, a big advantage of this new technique was revealed. It was concluded that for well optimized parameters, the joint never suffers a complete rupture and actually, stays connected and the joint's failure occurs like a regular tube extrusion. This comes as an advantage for any industrial application, where components are maintained connected in the event of a failure and obviously allows a safer and more predictable maintenance planning. Moreover, it was seen that the attained destructive loads were sensitive to the pull-out direction. The down-up direction presents smaller load values as it obliges the sheet to move in the direction of the already deformed tube, thus facilitating the pull-out test and lowering the loads.

Overall, it was possible to create and validate a new concept for Joining by Forming connection of sheets to tubes as long as the main defined parameters are respected. A single stroke process solves the lead time issues that other techniques shown in Chapter 2 caused.

A particular test was made using a Litecore sheet and an aluminium sheet, shown in Figure 7.1. As mentioned before, because the strength of the tube is larger than that of the sheet, the process doesn't work as the material flow tends be outwardly. However, what was observed in this particular test was slightly different than what expected. The material of the sheet (Litecore), instead of flowing outwardly, flowed downward, not creating any inner tube bead and failing to assure a connection between components.

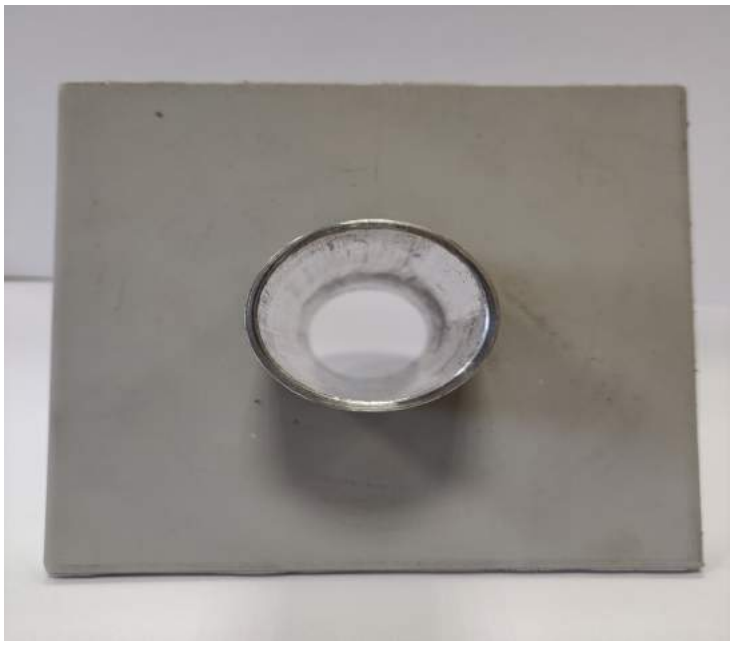

(a) Aluminium Tube and Litecore Sheet. No inner bead is formed thus the connection has failed.

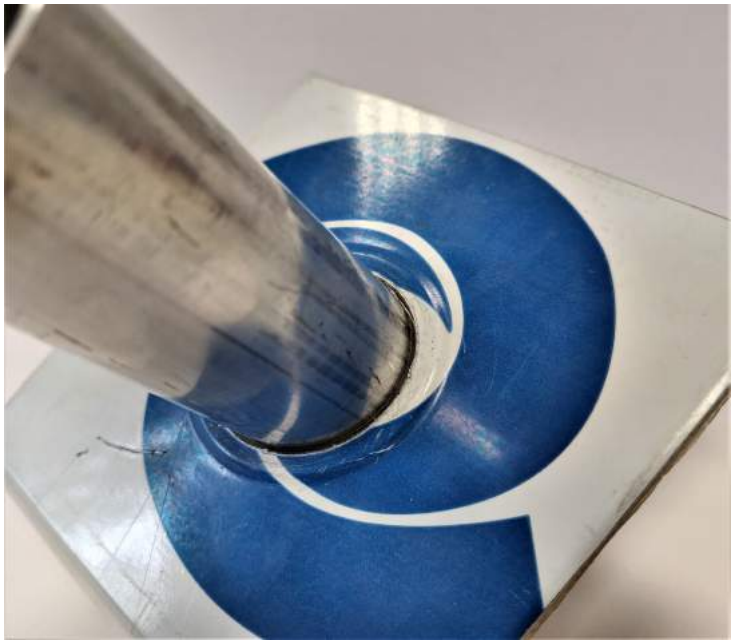

(b) Litecore Sheet downward flow problem.

Figure 7.1: Failed joining attempt of an aluminium tube and a Litecore sheet.

7.2 Future Work Perspectives

For further research on this new Joining by Forming technique, there are some aspects that would deserve attention and would validate this new concept even more.

When this new technique is used for sheets with larger thicknesses, it might be interesting to study the performance of joints performed by ”Spot Compression”. In other words, the process was only studied for squeezing punches that covered the tube's complete perimeter. Performing the compression in separated regions along the perimeter of the tube would allow smaller forming loads.

The inner tube bead shape might play an important role for numerous industrial situations, namely, in applications that implied the use of fluids inside the tube. In these cases, the existence of a large inner tube bead isn't desirable and in order to tackle that issue, the use of an inner mandrel would allow the control of the shape of the bead, optimizing this process for that kind of application. This dissertation doesn't cover that work and leaves the suggestion for a future work to be made regarding this particular aspect. Further investigation on different material combinations and different components, such as rods, is essential to widen the application window of this process. Moreover, this process has the potential to extend to other types of connections such has tube-to-tube and sheet-to-sheet connections. This work only studies the tube-to-sheet connections and the authors leave the future work suggestion. It would be an advantage for the technology proposed if a specific tool could be projected in order to increase portability and therefore possibilitate the use of the technology in situ. This dissertation provides an extensive study on the theoretical and technical aspects of this new technology. In order for an industrial integration to happen, a thorough study should be done in order to situate this new process in terms of implementation and operating costs, lead times and environmental impacts. It is agreed between the developers of this new technology that advantages are provided in all aspects mentioned above. However, having this information, further studies can be done in order to introduce this technology to industrial environments.

Bibliography

[1] Trumpf, "Enviromental impacts of welding methods," https://www.trumpf.com/pt_PT/revista/enviromental-impacts-of-welding-methods/, 2019, visited in 11/09/2019.

[2] L. M. Alves, E. J. Dias, and P. A. Martins, "Joining sheet panels to thin-walled tubular profiles by tube end forming," *Journal of Cleaner Production*, vol. 19, no. 6-7, pp. 712–719, 2011.

[3] K. Mori, N. Bay, L. Fratini, F. Micari, and A. E. Tekkaya, "Joining by plastic deformation," *CIRP Annals*, vol. 62, no. 2, pp. 673–694, 2013.

[4] P. Groche, S. Wohletz, M. Brenneis, C. Pabst, and F. Resch, "Joining by forming—a review on joint mechanisms, applications and future trends," *Journal of Materials Processing Technology*, vol. 214, no. 10, pp. 1972–1994, 2014.

[5] L. M. Alves, C. Silva, and P. A. Martins, "Joining by plastic deformation," in *Key Engineering Materials*, vol. 767. Trans Tech Publ, 2018, pp. 25–41.

[6] R. Matsumoto, S. Hanami, A. Ogura, H. Yoshimura, and K. Osakada, "New plastic joining method using indentation of cold bar to hot forged part," *CIRP annals*, vol. 57, no. 1, pp. 279–282, 2008.

[7] T. Altan and A. E. Tekkaya, *Sheet metal forming: processes and applications*. ASM international, 2012.

[8] F. Dohmann and K. Lange, "Innenhochdruckumformen, umformtechnik-handbuch für industrie und wissenschaft," 1993.

[9] G. Spur and T. Stöferle, *Handbuch der Fertigungstechnik: Fügen, Handhaben und Montieren*. Hanser Verlag, 1986, vol. 5.

[10] B. M. W. AG, *DE Patent 36 11 898 C1*, 1986.

[11] I. Sizova, A. Sviridov, and M. Bambach, "Avoiding crack nucleation and propagation during upset bulging of tubes," *International Journal of Material Forming*, vol. 10, no. 3, pp. 443–451, 2017.

[12] T. Reddy, “Guist and marble revisited—on the natural knuckle radius in tube inversion,” *International journal of mechanical sciences*, vol. 34, no. 10, pp. 761–768, 1992.

[13] P. Rosa, J. Rodrigues, and P. Martins, “External inversion of thin-walled tubes using a die: experimental and theoretical investigation,” *International Journal of Machine Tools and Manufacture*, vol. 43, no. 8, pp. 787–796, 2003.

[14] P. A. Rosa, J. M. Rodrigues, and P. A. Martins, “Internal inversion of thin-walled tubes using a die: experimental and theoretical investigation,” *International Journal of Machine Tools and Manufacture*, vol. 44, no. 7-8, pp. 775–784, 2004.

[15] P. A. Rosa, R. M. Baptista, J. M. Rodrigues, and P. A. Martins, “An investigation on the external inversion of thin-walled tubes using a die,” *International journal of plasticity*, vol. 20, no. 10, pp. 1931–1946, 2004.

[16] G. Sekhon, N. Gupta, and P. Gupta, “An analysis of external inversion of round tubes,” *Journal of Materials Processing Technology*, vol. 133, no. 3, pp. 243–256, 2003.

[17] L. Alves and P. Martins, “Single-stroke mechanical joining of sheet panels to tubular profiles,” *Journal of Manufacturing Processes*, vol. 15, no. 1, pp. 151–157, 2013.

[18] L. M. Alves and P. A. Martins, “Mechanical joining of tubes to sheets along inclined planes,” *steel research international*, vol. 83, no. 12, pp. 1135–1140, 2012.

[19] A. Gonçalves, L. M. Alves, and P. A. Martins, “Inclined tube-s heet plastically deformed joints,” *steel research international*, vol. 85, no. 1, pp. 67–75, 2014.

[20] L. Alves, J. Gameiro, C. Silva, and P. Martins, “Sheet-bulk forming of tubes for joining applications,” *Journal of Materials Processing Technology*, vol. 240, pp. 154–161, 2017.

[21] P. Sieczkarek, L. Kwiatkowski, N. Ben Khalifa, and A. E. Tekkaya, “Novel five-axis forming press for the incremental sheet-bulk metal forming,” in *Key Engineering Materials*, vol. 554. Trans Tech Publ, 2013, pp. 1478–1483.

[22] M. Merklein, A. E. Tekkaya, A. Brosius, S. Opel, L. Kwiatkowski, B. Plugge, and S. Schunk, “Machines and tools for sheet-bulk metal forming,” in *Key Engineering Materials*, vol. 473. Trans Tech Publ, 2011, pp. 91–98.

[23] M. Merklein, J. Allwood, B.-A. Behrens, A. Brosius, H. Hagenah, K. Kuzman, K. Mori, A. Tekkaya, and A. Weckenmann, “Bulk forming of sheet metal,” *CIRP annals*, vol. 61, no. 2, pp. 725–745, 2012.

[24] L. Alves, R. Afonso, C. Silva, and P. Martins, “Boss forming of annular flanges in thin-walled tubes,” *Journal of Materials Processing Technology*, vol. 250, pp. 182–189, 2017.

[25] ——, “Joining sandwich composite panels to tubes,” *Proceedings of the Institution of Mechanical Engineers, Part L: Journal of Materials: Design and Applications*, p. 1464420718763463, 2018.

[26] ——, “Joining tubes to sheets by boss forming and upsetting,” *Journal of Materials Processing Technology*, vol. 252, pp. 773–781, 2018.

[27] L. M. Alves, R. M. Afonso, C. Silva, and P. A. Martins, “Joining by forming of tubes to sheets with counterbored holes,” in *Key Engineering Materials*, vol. 767. Trans Tech Publ, 2018, pp. 421–428.

[28] L. M. Alves, F. L. Silva, R. M. Afonso, and P. A. Martins, “Joining sheets to tubes by annular sheet squeezing,” *International Journal of Machine Tools and Manufacture*.

[29] ——, “A new joining by forming process for fixing sheets to tubes,” *International Journal of Advanced Manufacturing Technology*.

[30] R. Caddell and A. G. Atkins, “The influence of redundant work when drawing rods through conical dies,” *Journal of Engineering for Industry*, vol. 90, no. 2, pp. 411–416, 1968.

[31] R. Hill, *The mathematical theory of plasticity*. Oxford university press, 1998, vol. 11.

[32] L. M. Alves, R. M. Afonso, F. L. Silva, and P. A. Martins, “Deformation assisted joining of sheets to tubes by annular sheet squeezing,” 2019.